NUREG/ CR-2880
PNL-4307

Acoustic Emission Monitoring of ASME Section III Hydrostatic Test

Watts Bar Unit 1 Nuclear Reactor

Prepared by P. H. Hutton, T. T. Taylor, J. F. Dawson,
R. A. Pappas, R. J. Kurtz

Pacific Northwest Laboratory
Operated by
Battelle Memorial Institute

Prepared for
U.S. Nuclear Regulatory
Commission

Availability of Reference Materials Cited in NRC Publications

Most documents cited in NRC publications will be available from one of the following sources:

1. The NRC Public Document Room, 1717 H Street, N.W. Washington, DC 20555
2. The NRC/GPO Sales Program, U.S. Nuclear Regulatory Commission, Washington, DC 20555
3. The National Technical Information Service, Springfield, VA 22161

Although the listing that follows represents the majority of documents cited in NRC publications, it is not intended to be exhaustive.

Referenced documents available for inspection and copying for a fee from the NRC Public Document Room include NRC correspondence and internal NRC memoranda; NRC Office of Inspection and Enforcement bulletins, circulars, information notices, inspection and investigation notices; Licensee Event Reports; vendor reports and correspondence; Commission papers; and applicant and licensee documents and correspondence.

The following documents in the NUREG series are available for purchase from the NRC/GPO Sales Program: formal NRC staff and contractor reports, NRC-sponsored conference proceedings, and NRC booklets and brochures. Also available are Regulatory Guides, NRC regulations in the *Code of Federal Regulations*, and *Nuclear Regulatory Commission Issuances*.

Documents available from the National Technical Information Service include NUREG series reports and technical reports prepared by other federal agencies and reports prepared by the Atomic Energy Commission, forerunner agency to the Nuclear Regulatory Commission.

Documents available from public and special technical libraries include all open literature items, such as books, journal and periodical articles, and transactions. *Federal Register* notices, federal and state legislation, and congressional reports can usually be obtained from these libraries.

Documents such as theses, dissertations, foreign reports and translations, and non-NRC conference proceedings are available for purchase from the organization sponsoring the publication cited.

Single copies of NRC draft reports are available free upon written request to the Division of Technical Information and Document Control, U.S. Nuclear Regulatory Commission, Washington, DC 20555

Copies of industry codes and standards used in a substantive manner in the NRC regulatory process are maintained at the NRC Library, 7920 Norfolk Avenue, Bethesda, Maryland, and are available there for reference use by the public. Codes and standards are usually copyrighted and may be purchased from the originating organization or, if they are American National Standards, from the American National Standards Institute, 1430 Broadway, New York, NY 10018.

GPO Printed copy price: $4.75

NUREG/CR-2880
PNL-4307
R5, GS

Acoustic Emission Monitoring of ASME Section III Hydrostatic Test

Watts Bar Unit 1 Nuclear Reactor

Manuscript Completed: June 1982
Date Published: October 1982

Prepared by
P. H. Hutton, T. T. Taylor, J. F. Dawson
R. A. Pappas, R. J. Kurtz

Pacific Northwest Laboratory
Richland, WA 99352

Prepared for
Division of Engineering Technology
Office of Nuclear Regulatory Research
U.S. Nuclear Regulatory Commission
Washington, D.C. 20555
NRC FIN B2088

ABSTRACT

Through the cooperation of the Tennessee Valley Authority, Pacific Northwest Laboratory has installed instrumentation on Watts Bar Nuclear Power Plant Unit 1 for the purpose of test and evaluation of acoustic emission (AE) monitoring of nuclear reactor pressure vessels and piping for flaw detection.

This report describes the acoustic emission monitoring performed during the ASME Section III hydrostatic testing of Watts Bar Nuclear Power Plant Unit 1 and the results obtained. Highlights of the results are:

- Spontaneous AE was detected from a nozzle area during final pressurization.
- Evaluation of the apparent source of the spontaneous AE using an empirically derived AE/fracture mechanics relationship agreed within a factor of two with an evaluation by ASME Section XI Code procedures.
- AE was detected from a fracture specimen which was pressure coupled to the 10-inch accumulator nozzle. This provided reassurance of adequate system sensitivity.
- High background noise was observed when all four reactor coolant pumps were operating.

Work is continuing at Watts Bar Unit 1 toward AE monitoring hot functional testing and subsequently monitoring during reactor operation.

CONTENTS

LIST OF FIGURES

ACOUSTIC EMISSION MONITORING
OF
ASME SECTION III HYDROSTATIC TEST
WATTS BAR UNIT 1 NUCLEAR REACTOR*

1.0 INTRODUCTION

Pacific Northwest Laboratory (PNL) is performing a research program for the U.S. Nuclear Regulatory Commission (NRC) with the objective of experimentally evaluating the feasibility of detecting and analyzing flaw growth in nuclear reactor pressure boundaries by means of acoustic emission (AE) monitoring. As part of this program, a demonstration of on-line reactor monitoring is required.

The on-line reactor monitoring demonstration has been divided into three phases:

- AE monitoring during a cold hydrostatic test,
- AE monitoring during hot functional testing, and
- AE monitoring during reactor startup and power operation.

Through the cooperation of the Tennessee Valley Authority (TVA), PNL has installed instrumentation on Watts Bar Nuclear Power Plant Unit 1 for the purpose of test and evaluation of on-line AE monitoring.

This report presents the results from AE monitoring of the ASME Section III cold hydrostatic test.

*Work supported by the U.S. Nuclear Regulatory Commisstion under Contract No. DEAC06-76-RLO 1830, Fin. No. B2088; NRC Contact: Dr. J. Muscara.

2.0 SELECTION OF MONITORING AREAS

With the concurrence of the cognizant TVA, NRC, and PNL personnel, the following three areas of the Watts Bar Unit 1 nuclear facility were instrumented for AE monitoring.

- Inlet nozzle No. 2 on reactor coolant loop,
- The loop 2 accumulator piping at the point of injection into loop 2 cold leg, and
- A section of the reactor pressure vessel between the loop 2 inlet and outlet nozzles.

Inlet nozzle No. 2 was chosen because preservice ultrasonic examinations had revealed small indications in the nozzle due to underclad cracking.*

In addition to instrumenting an area with known defects, a fatigue precracked fracture specimen was strapped to the 10-inch accumulator injection pipe on the loop 2 cold leg. The fracture specimen included a small hydraulic ram to facilitate growth of the crack during cold hydrostatic testing to produce known AE. The purpose of the fracture specimen was to demonstrate that the acoustic emission technique could detect cracking during conditions which begin to approximate plant operating conditions.

The section of vessel wall is being monitored to help assess the feasibility of AE monitoring the vessel belt line fabrication weld with sensors at the closest readily accessible locations on the vessel.

*Several crack like indications around inlet nozzle No. 2 were detected during preservice examinations. The larger defects were repaired and only defects allowable under Section XI remain.

3.0 TEST EQUIPMENT AND INSTALLATION

The AE equipment used for monitoring the Watts Bar hydrostatic test consisted of tuned sensors, signal conditioners, a spectrum analyzer, and a Dunegan/Endevco 1032D data acquisition system. Waveform recording and pattern recognition instrumentation which comprises the balance of the planned system for reactor monitoring were not utilized because the short notice of test start-up precluded shipping the instruments to the reactor site.

Each sensor consists of a 1/8 inch diameter stainless steel waveguide with differential sensing element and a 20 dB differential amplifying circuit mounted on one end. The other end of the waveguide is pressure coupled to the reactor surface using magnets or metal straps. The sensor is tuned with a bandwidth of approximately 300-400 kHz and a peak response frequency of approximately 375 kHz. The frequency range above 300 kHz was used for monitoring to avoid the large background noise associated with lower frequencies.(1) Further signal conditioning and an additional 20 dB of gain are achieved with separate "midamplifiers" prior to signal input to the Dunegan/Endevco 1032D system.

The Dunegan/Endevco 1032D data acquisition system which receives the output from the sensor assemblies is microprocessor controlled. Acoustic emission events are detected and characterized by signal processing circuit boards. The resulting data are displayed and also stored on floppy disks to be accessed for post-test analysis. A more detailed description of the Dunegan/Endevco 1032D data acquisition system is presented in Appendix I.

A total of 11 sensors and a mechanical impactor were installed on the No. 2 inlet nozzle. Figure 1 is a diagram of the sensor layout. The waveguides were pressure coupled to the vessel using a magnetic mounting technique. Placement of some of the sensors required that the stainless steel insulating shroud around the vessel be modified. The sections of waveguide immediately protruding from the sensor box were magnetically fixed to the biological shield to meet seismic safety constraints. Delrin sleeving prevented the waveguides from contacting the steel liner of the biological shield. The impactor is a small solenoid controlled device used to create a transient signal in the material to which it is attached. Detection of this signal gives a relative measure of AE system functional integrity.

Six sensors and a precracked test specimen were located on the safety injection line. Again, the waveguides were pressure

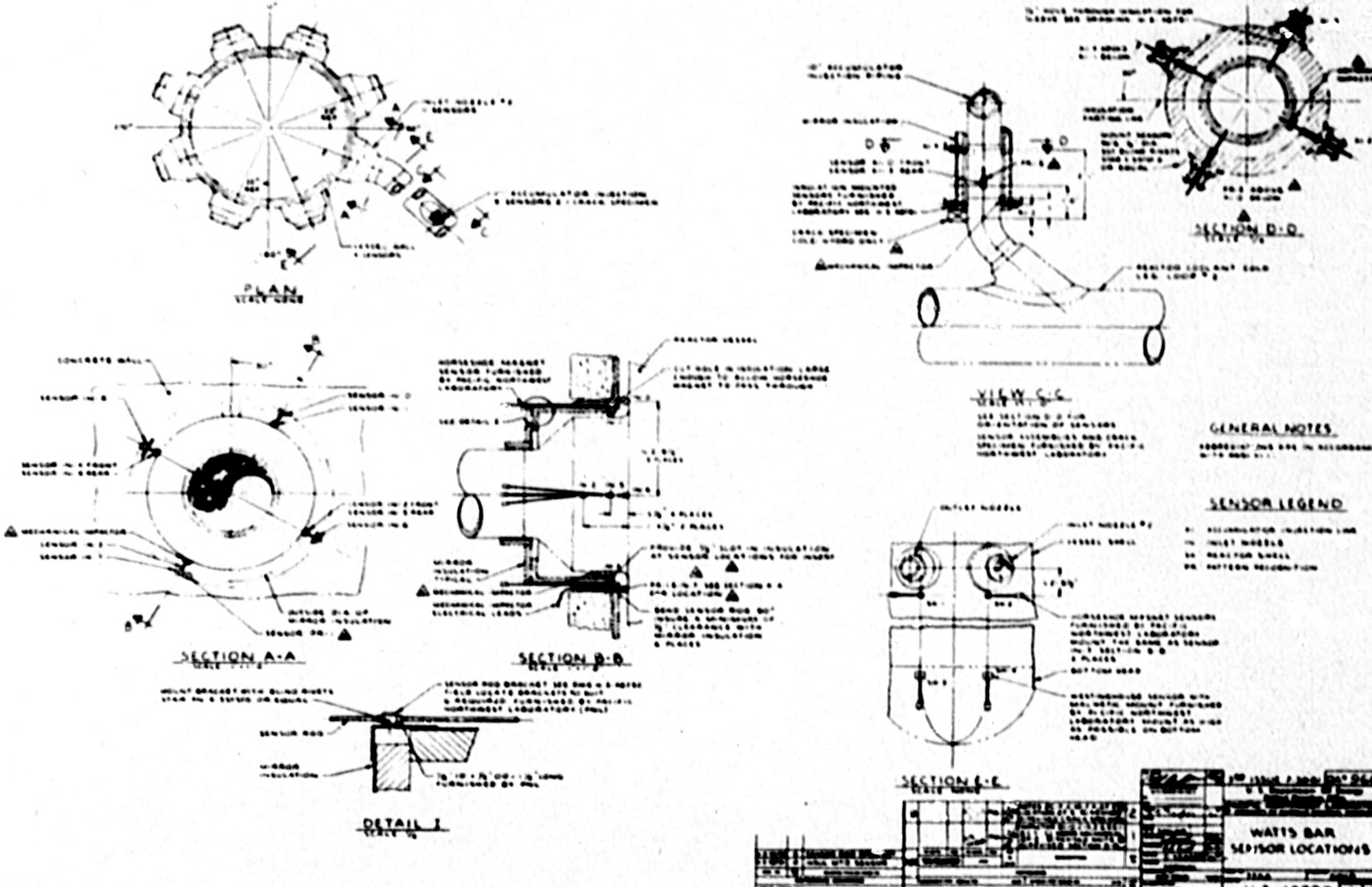

Figure 1. Diagram of Sensor Location.

coupled to the piping. Delrin sleeving was used to prevent acoustic coupling between waveguides and mounting brackets. The precracked test specimen was held in place with stainless steel banding and a viscous ultrasonic couplant was used to couple the specimen to the pipe.

One rectangular AE sensing array was set up on the reactor vessel. Two magnetically mounted Westinghouse high temperature sensors were attached 57 inches from the bottom of the vessel at 115° and 160° azimuth. A 3 in. x 3 in. hole was cut in the vessel shroud at the outlet nozzles in the No. 2 loop to facilitate installing a waveguide sensor for one upper corner of the array. One of the sensors installed on the inlet nozzle of loop 2 was used in a dual capacity to form the other upper corner of the vessel array and also served as part of a nozzle monitor array.

The mid-amplifiers, D/E data acquisition system, and the 1032D computer were located outside of containment in the pipe galley at 20° azimuth. It was, therefore, necessary to lay 250 feet of temporary RG-58 cable for each sensor. For the two Westinghouse sensors, four lengths of high temperature RG-141 cable were run.

4.0 TEST CONDITIONS

In order to better understand the acquisition of data, a brief description of the mechanics of the cold hydrostatic follows.

The cold hydrostatic test is performed as part of the fabrication requirements of Section III of the ASME Boiler and Pressure Vessel Code. Section III requires that all Class 1 pressure retaining components be hydrostatically tested prior to initial operation. The nominal test pressure is required to be 1.25 times the design pressure of the system.

At Watts Bar the cold hydrostatic test was conducted in several major steps which were:

- Initial valve line up.
- Fill and vent primary system.
- Pressurize to 300 psig and hold to check for leaks and test water chemistry. Run reactor coolant pumps to achieve test temperature.
- Pressurize to 700 psig and hold for water chemistry.
- Pressurize to 1500 psig. Hold for water chemistry. Change valve line up to allow further pressurizing with positive displacement charging pump.
- Pressurize to 2485 psig (design pressure). Hold for water chemistry.
- Pressurize to 3150 psig (test pressure). Hold for required test time (10 minutes).
- De-pressurize to 2485 psig and visually inspect system for leakage and structural distress.

The time required to perform the test from initial valve line up to final walk through was approximately nine days.

The variety of operating conditions that occurred during the test allowed valuable data to be acquired in terms of:

- Wide ranges of background noise, both electrical and hydraulic.
- Varying data rates resulting from pumps being turned on and off, system pressurization and hold periods.

Two significant factors affected data acquisition. First, the two high temperature Westinghouse sensors and the sensor on loop 2 outlet nozzle were inoperative due to damage sustained between installation and the test. This eliminated monitoring the vessel wall except for a limited area around loop 2 inlet nozzle.

Second, with all reactor coolant pumps operating, the perceived background noise was quite high. The decision was made to use only linear arrays for test monitoring because the sensors were closer together and less subject to missing signals due to noise interference. Three linear arrays were used on loop 2 inlet nozzle and one linear array was used on the 10-inch accumulator injection pipe.

5.0 TEST RESULTS

The results considered to be of primary importance to be discussed are:

- Background noise from coolant pumps.
- Detection of AE from fracture specimen.
- Filtering electrical transients.
- Spontaneous AE detected.

5.1 COOLANT PUMP NOISE

The background noise due to operation of the primary coolant pumps affected the AE monitor system more than expected during initial heatup and pressurization of the reactor system. Measured directly from the sensing system on an oscilloscope, the background noise with 70 dB of system gain was 18 volts peak-to-peak at the accumulator injection pipe and 12 volts peak-to-peak at the vessel inlet nozzle. These measurements are shown in Figure 2. Spectral characterization of the measured background noise were used to estimate the true character of the background noise. The results are shown in Figures 3 and 4. Appendix II details the method used in analyzing the frequency spectrum. The spectral characteristics of the background noise are similar to that reported by previous investigators,[1,2] however, the magnitude is greater. Figure 5 shows the spectral data obtained from measurements made at San Onofre Nuclear Power Plant. One factor which may be significant to the high noise levels observed during this test is the fact that the vessel contained no inner structure as it will later. This could serve to reinforce the pump noise.

5.2 AE FROM FRACTURE SPECIMEN AND ELECTRICAL TRANSIENTS

A precracked test specimen of heat treated 4340 steel was mounted on the safety injection pipe to loop 2 cold leg for the purpose of injecting known crack growth AE signals into the structure for AE system detection testing. The specimen was acoustically coupled to the pipe using a viscous ultrasonic coupling fluid. Low fracture toughness 4340 steel was used to help assure crack growth under the constraints of specimen mounting and loading methods.

AE from growing the crack in the specimen (ultimately cracking to failure) was detectable. In addition, it served to demonstrate the effectiveness of signal duration filtering to eliminate spike electrical transients from the data.

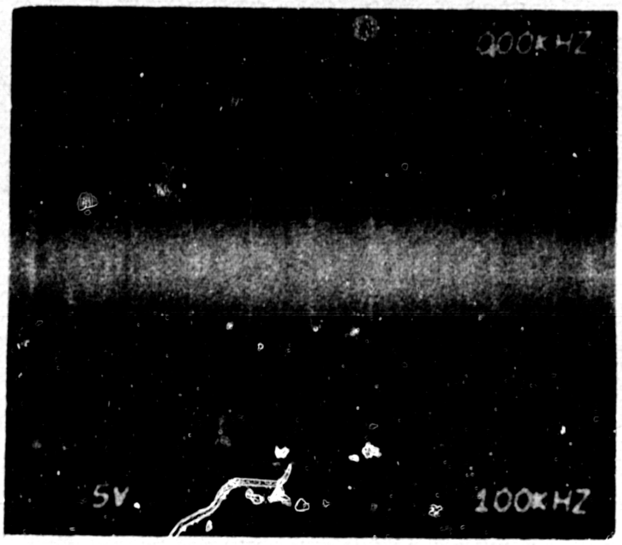

Background noise at accumulator injection pipe with all reactor pumps operating

- 40 dB gain into 2 sensor Battelle NRC system
- Total system gain = 70 dB

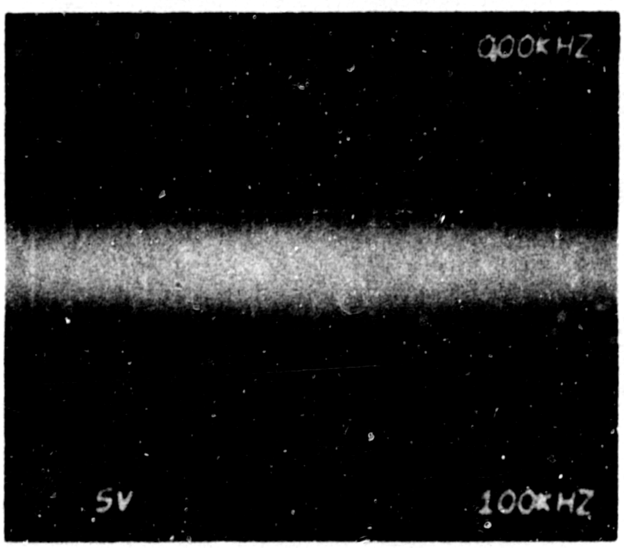

Background noise at inlet nozzle on vessel with all reactor coolant pumps operating

- 40 dB gain into 2 sensor Battelle NRC system
- Total system gain = 70 dB

Figure 2. Background Noise Amplitude in Volts Peak/Peak.

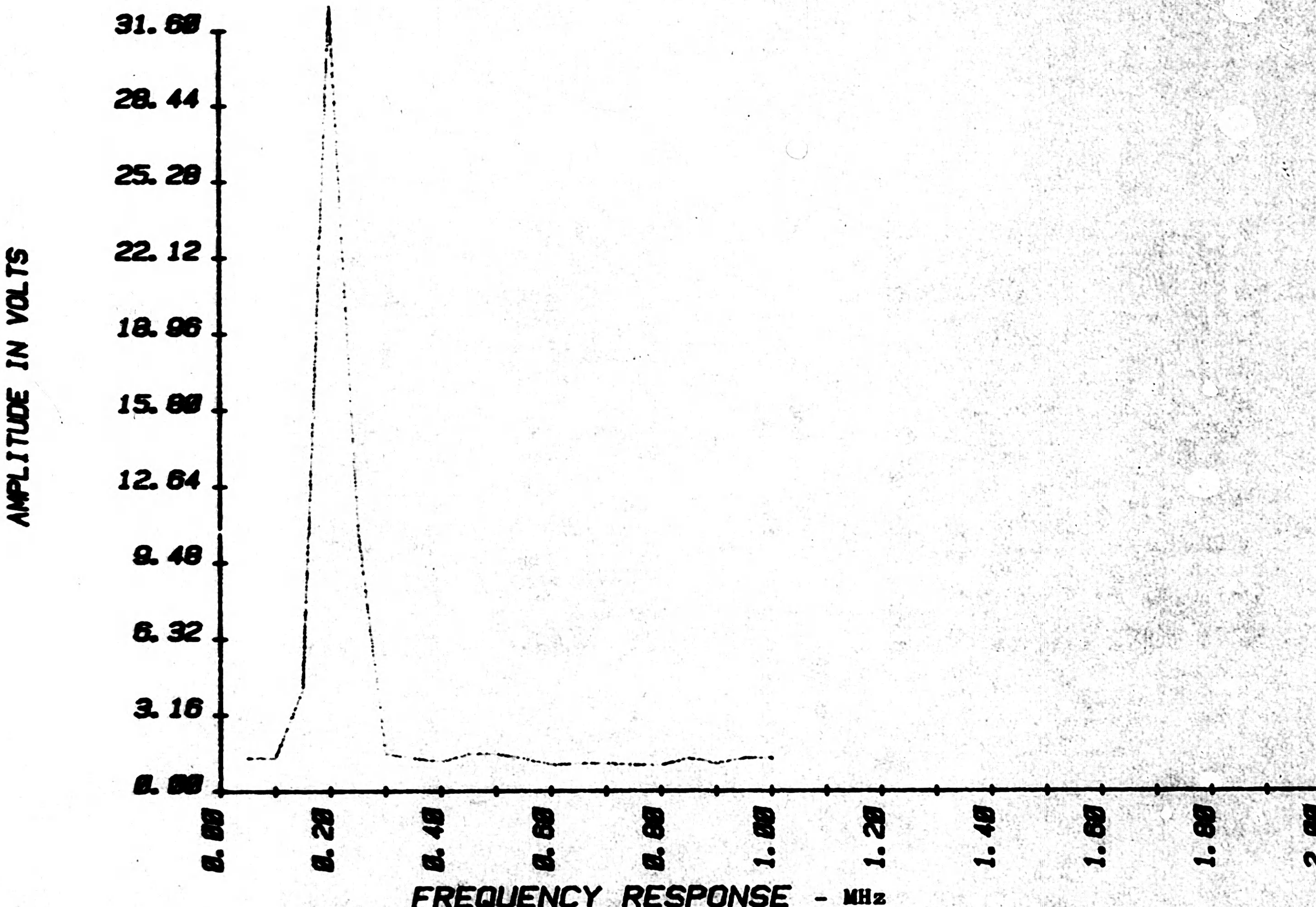

Figure 3. Background Noise Spectra at Accumulator Injection Pipe.

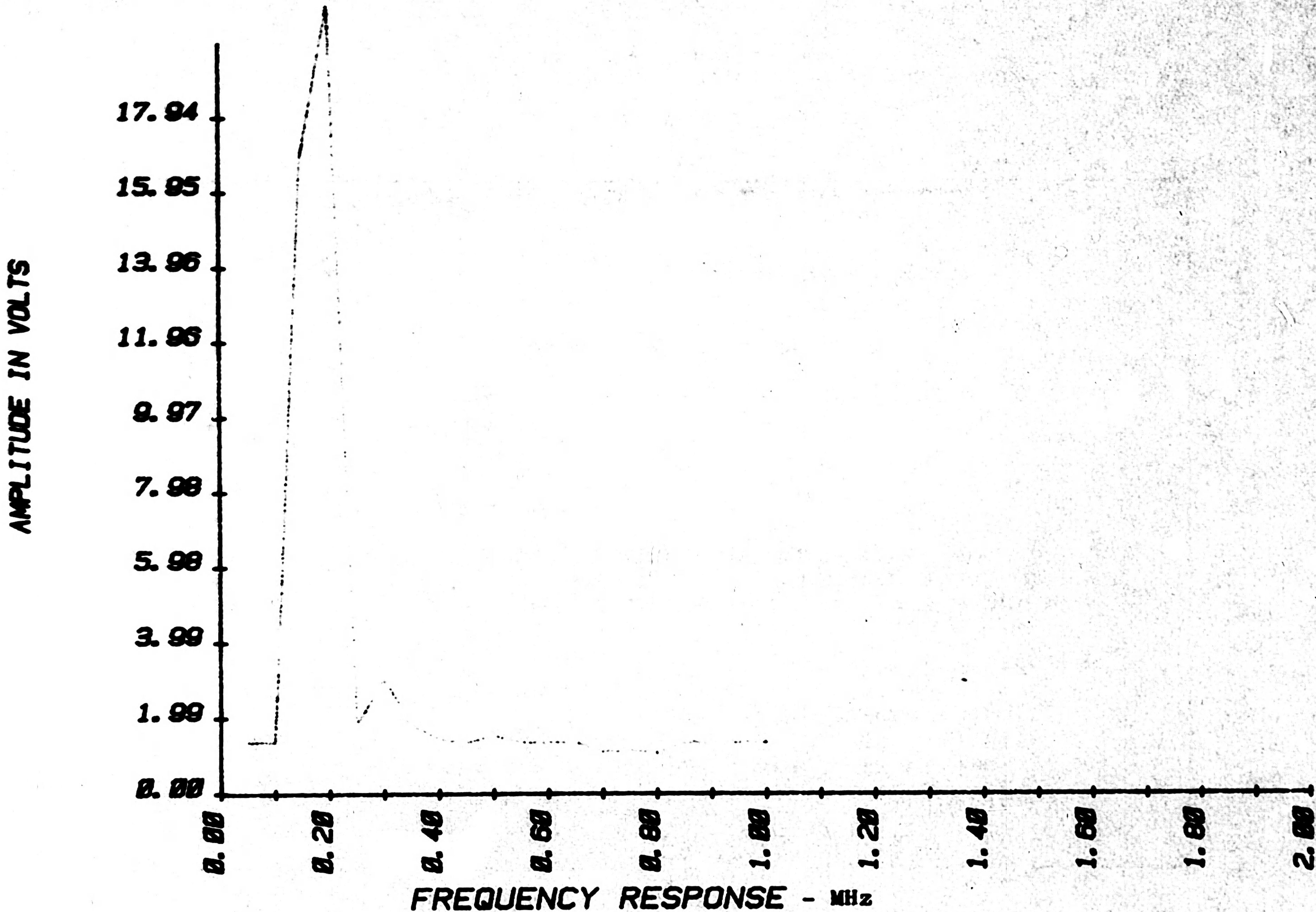

Figure 4. Background Noise Spectra at Vessel Nozzle.

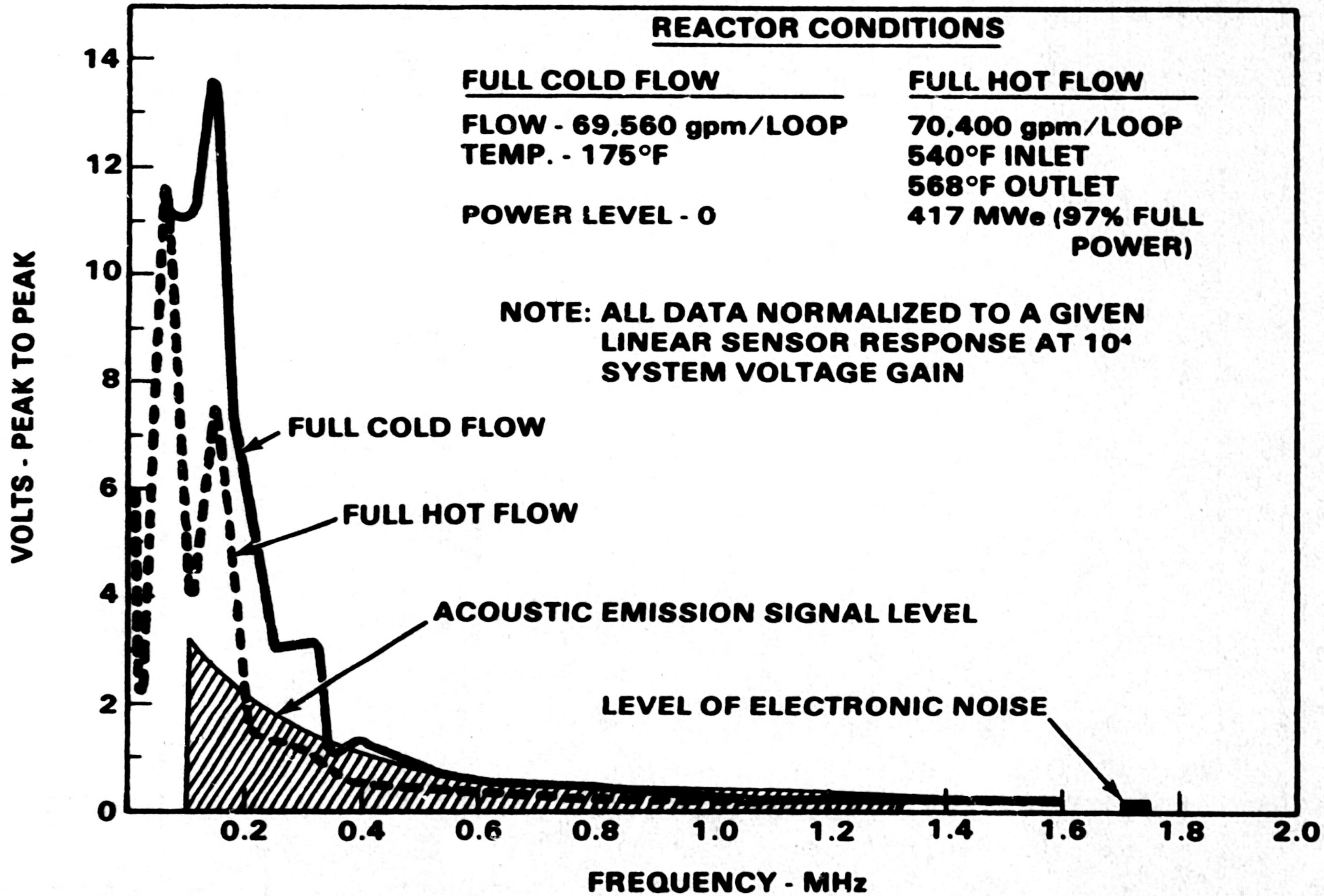

Figure 5. Background Noise Spectra Measured at San Onofre Nuclear Power Plant, Unit 1.

During the course of the hydrostatic test, construction welding continued. This had the effect of producing many spike transient signals. In fact, electrical spikes from the welding were so numerous that the cold hydro test data occupied two digital recording disks. File (disk) 1 contained crack specimen data and initial pressurization (to design pressure) data. File 2 contains data from final pressurization, hold period and depressurization. The plots in Figures 6 and 7 show the effects of the electrical transients on the overall data profile. Representative signal duration distribution for the gross data is shown in Figure 8. Signal duration distribution for AE signals from the fracture specimen is shown in Figure 9. Most of the signals fall within the range of 0.1 to 1.0 milliseconds. If a signal duration filter of 0.1 to 1.0 milliseconds is applied to the gross data, the result is as shown in Figures 10 and 11 where essentially all of the spike transients have been removed. This is a technique we plan to use in conjunction with pattern recognition methods to identify AE signals from crack growth. Although pattern recognition is very effective in rejecting spurious electrical spikes, duration filtering is a much simpler method that can be used to reduce the data processing load on the pattern recognition system.

5.3 SPONTANEOUS AE DETECTED

The crucial intervals of monitoring were the final pressure ascent from design to test pressure, the ten-minute hold at test pressure, and the beginning of the pressure drop. During this period, attention was focused on the No. 2 inlet nozzle area (as pointed out earlier, the vessel wall array had been rendered inoperative). The possibility of very high background noise as reactor coolant pumps were turned on and off to maintain temperature during testing influenced the decision to monitor using four two-sensor linear arrays. Because linear arrays were used, point source location was not possible; only relative areas of activity could be defined. Figure 12 shows the location of the sensor arrays on the No. 2 inlet nozzle.

The total data measured during final pressurization (spike transients less than 0.1 millisecond duration filtered out) is plotted in Figure 13. When this is compared with the associated hydro test pressure curve in Figure 14, there is a very rational correlation between the two. The number of AE counts is quite small and the rate of increase drops to practically zero before the pressure hold is completed. Note: Due to the circumstances of the test, the time scale on the pressure curve may lag actual time by as much as five minutes.

Looking in further detail at the distribution of the total AE among the three arrays on the No. 2 nozzle, we find (Figure

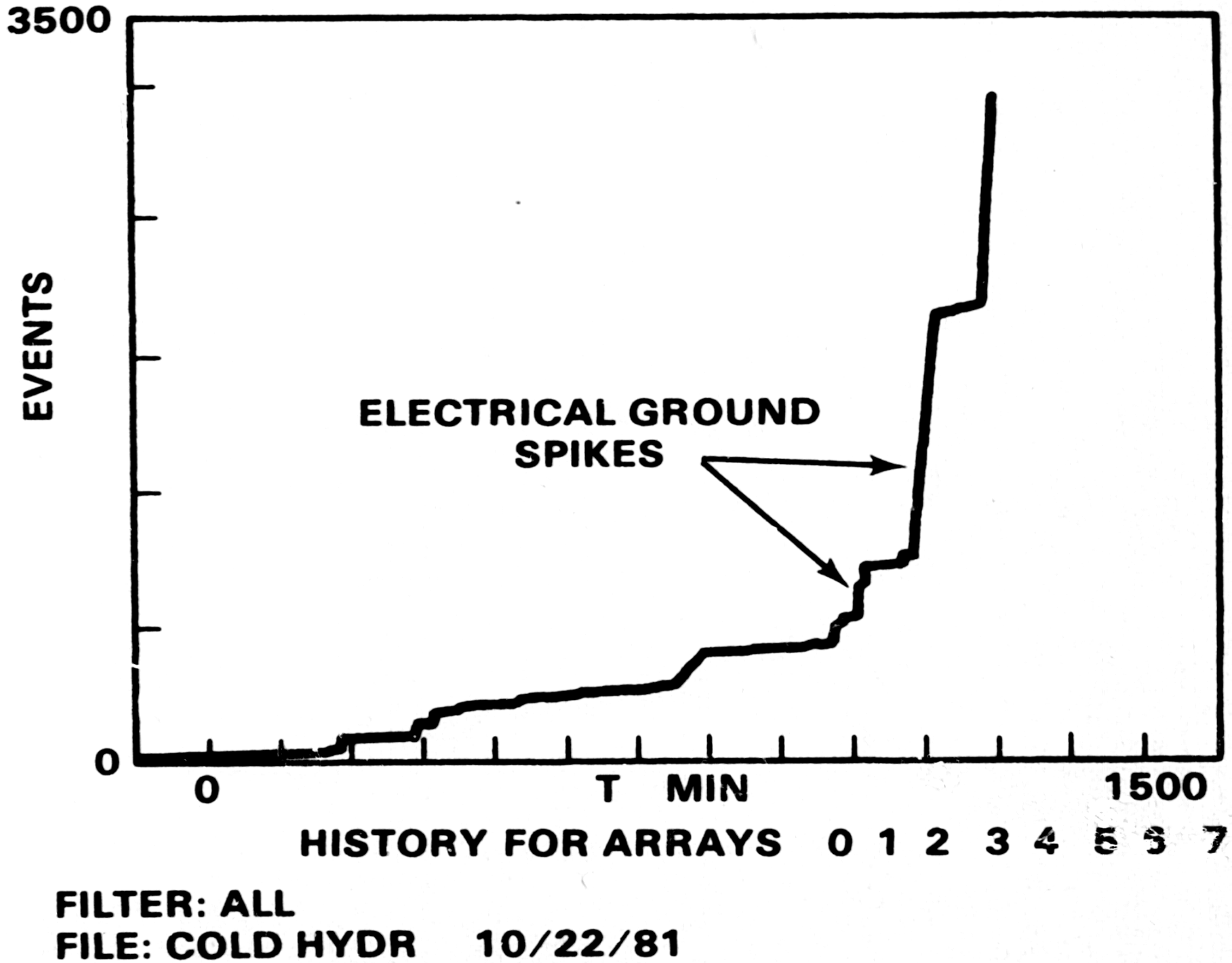

Figure 6. Cumulative Number of Events as a Function of Time for Data File 1.

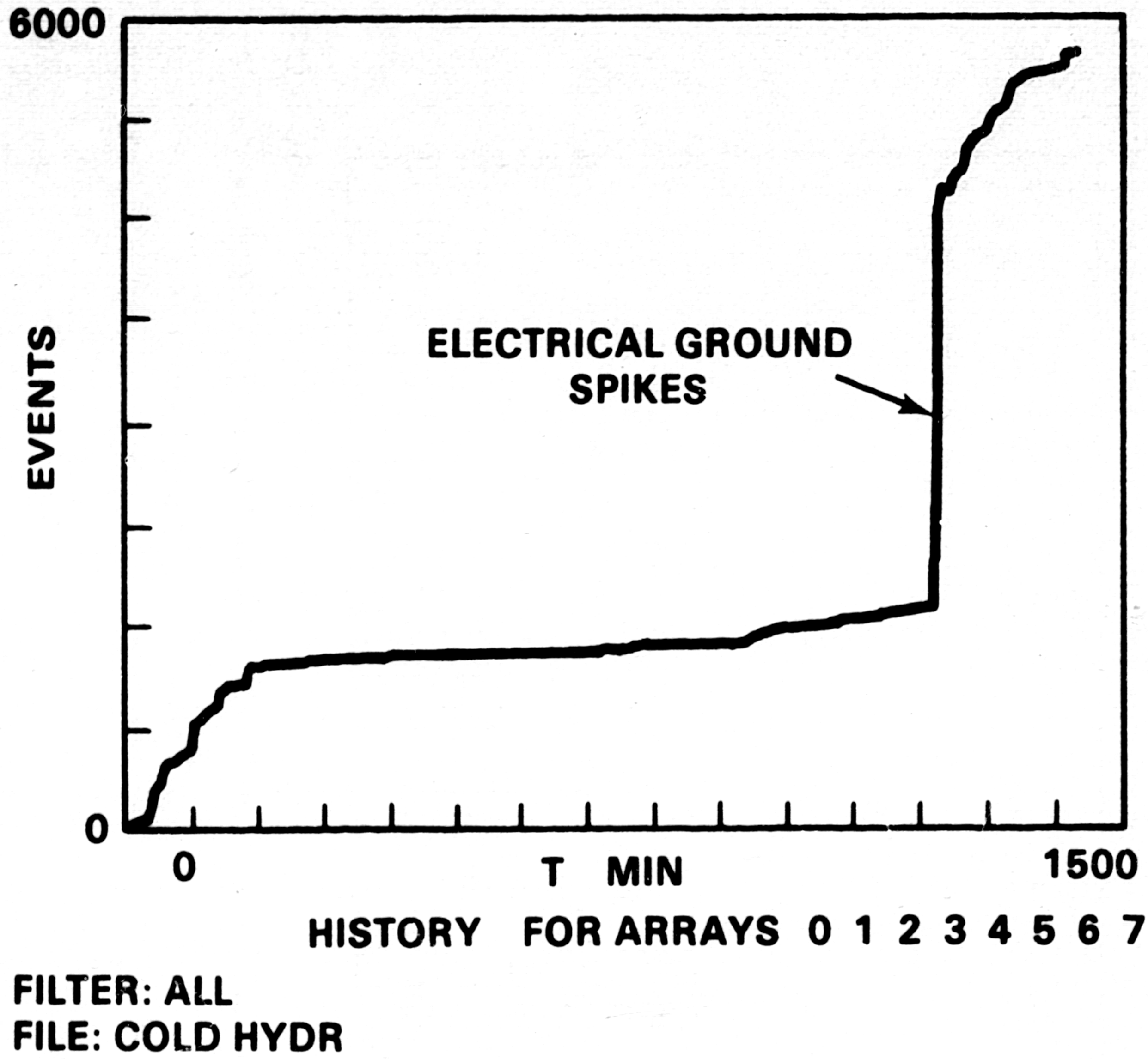

Figure 7. Cumulative Number of Events as a Function of Time for Data File 2.

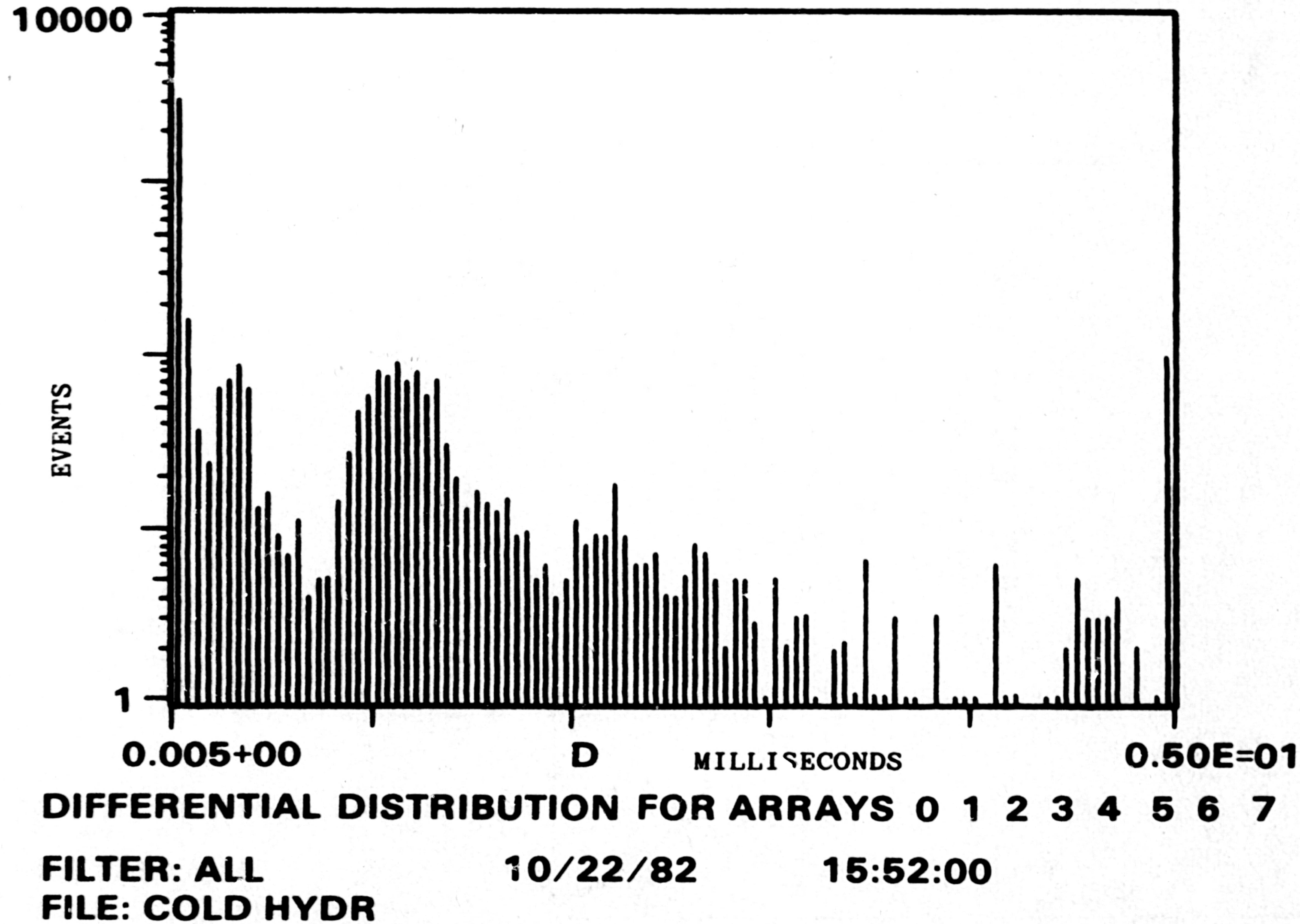

Figure 8. Signal Duration Distribution for All Events in Data File 1.

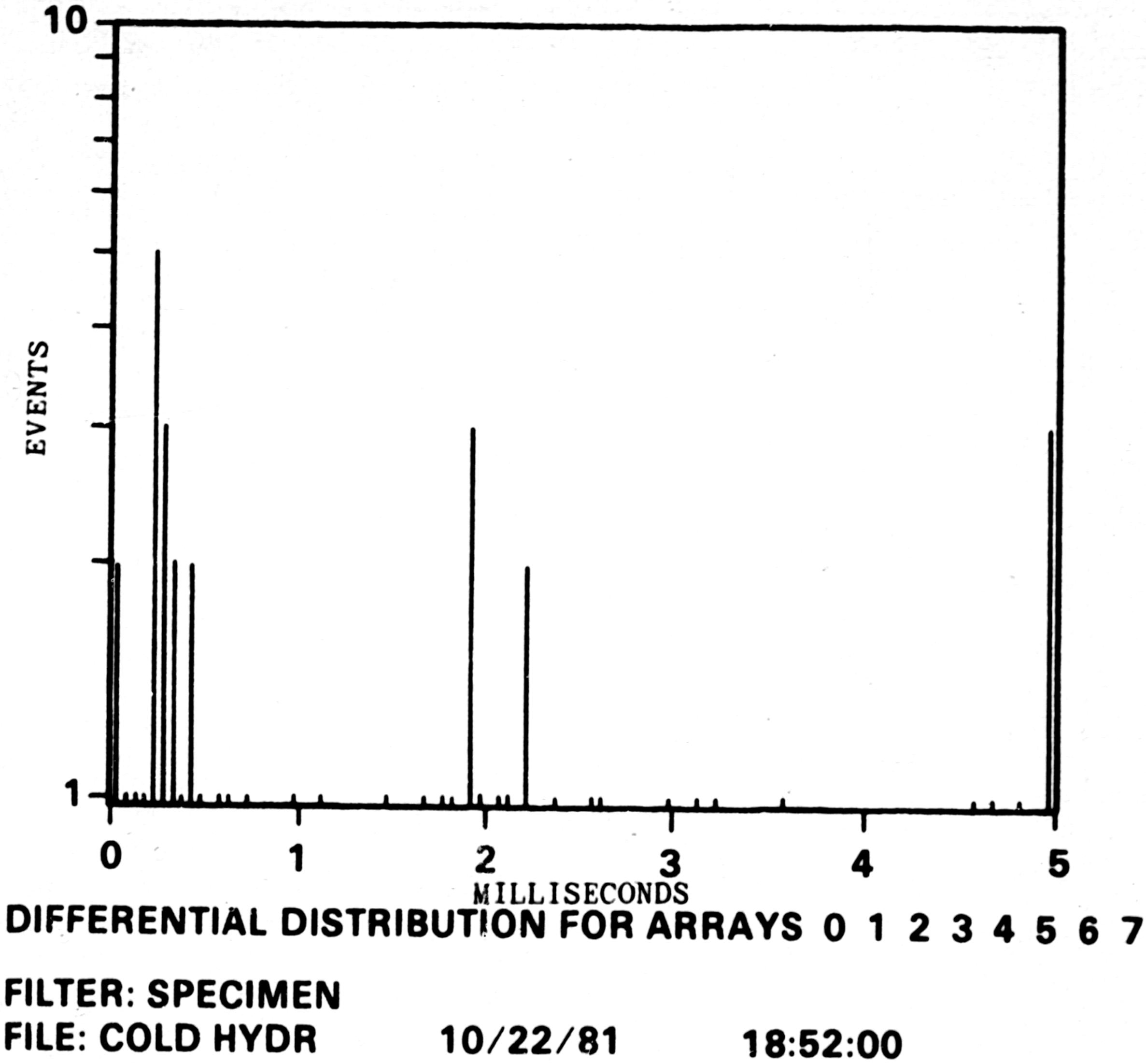

Figure 9. Signal Duration Distribution for Events from Fracture Specimen Failure.

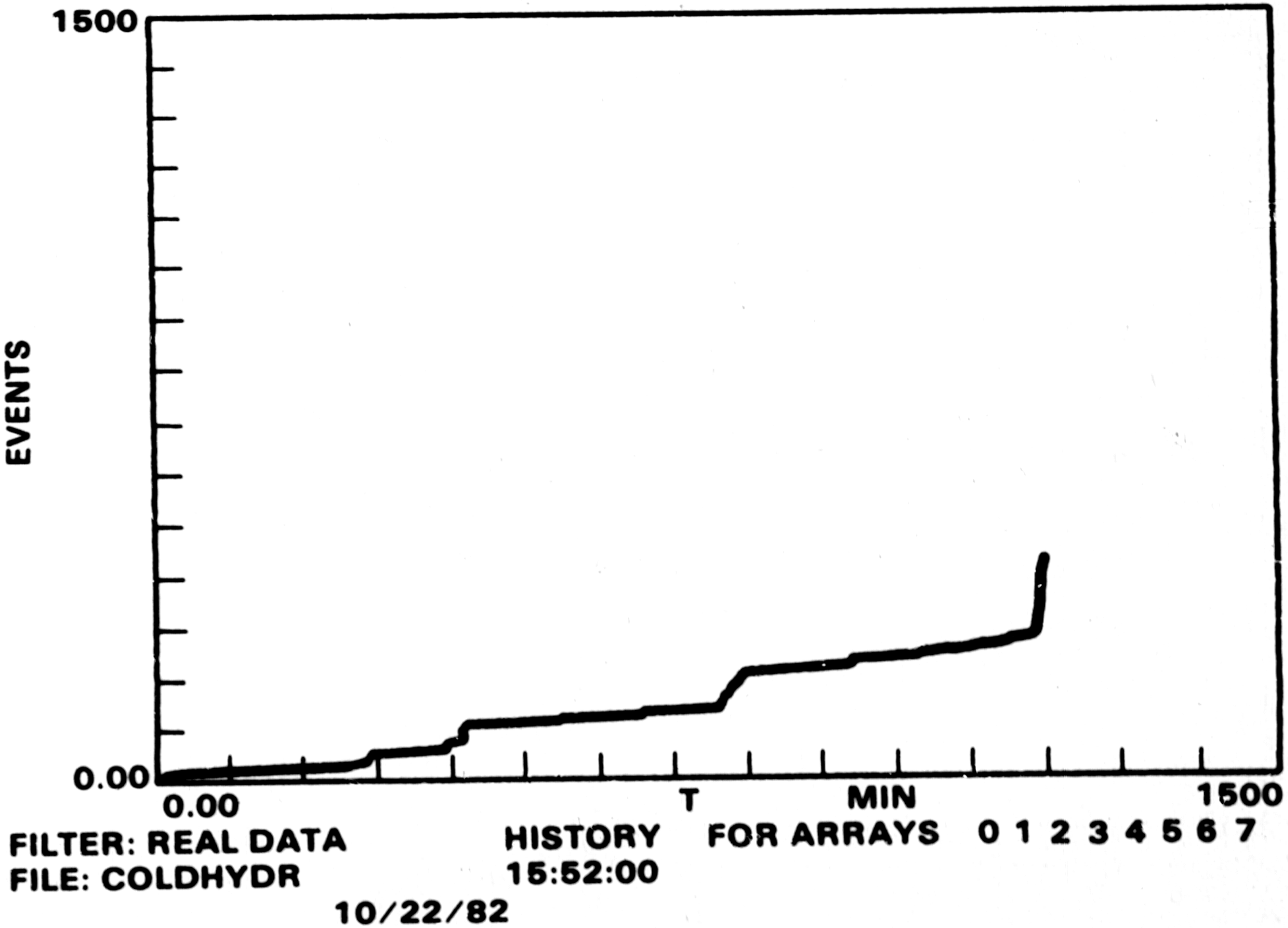

Figure 10. Filtered Events Versus Time for Data File 1.

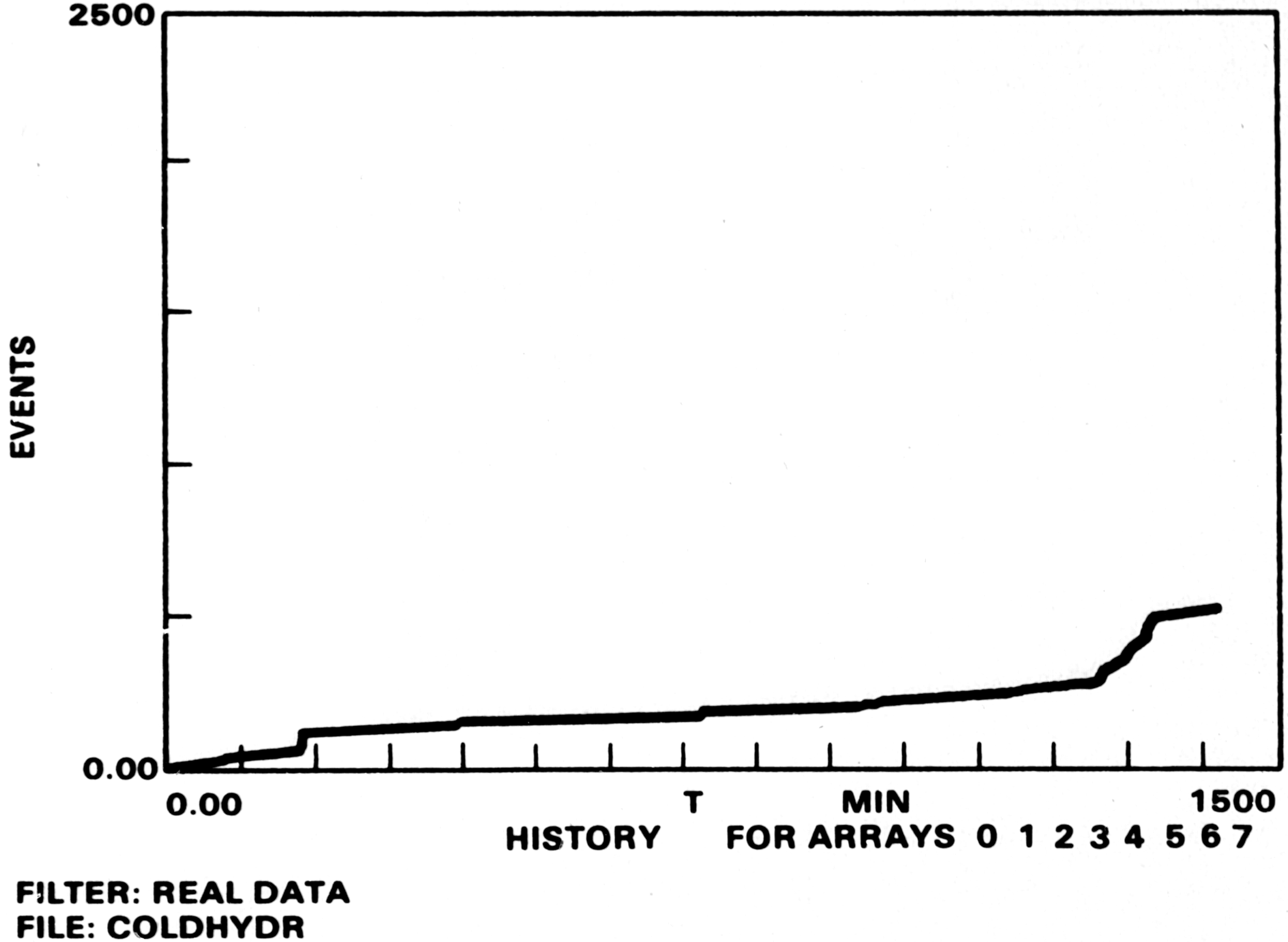

Figure 11. Filtered Events Versus Time for Data File 2.

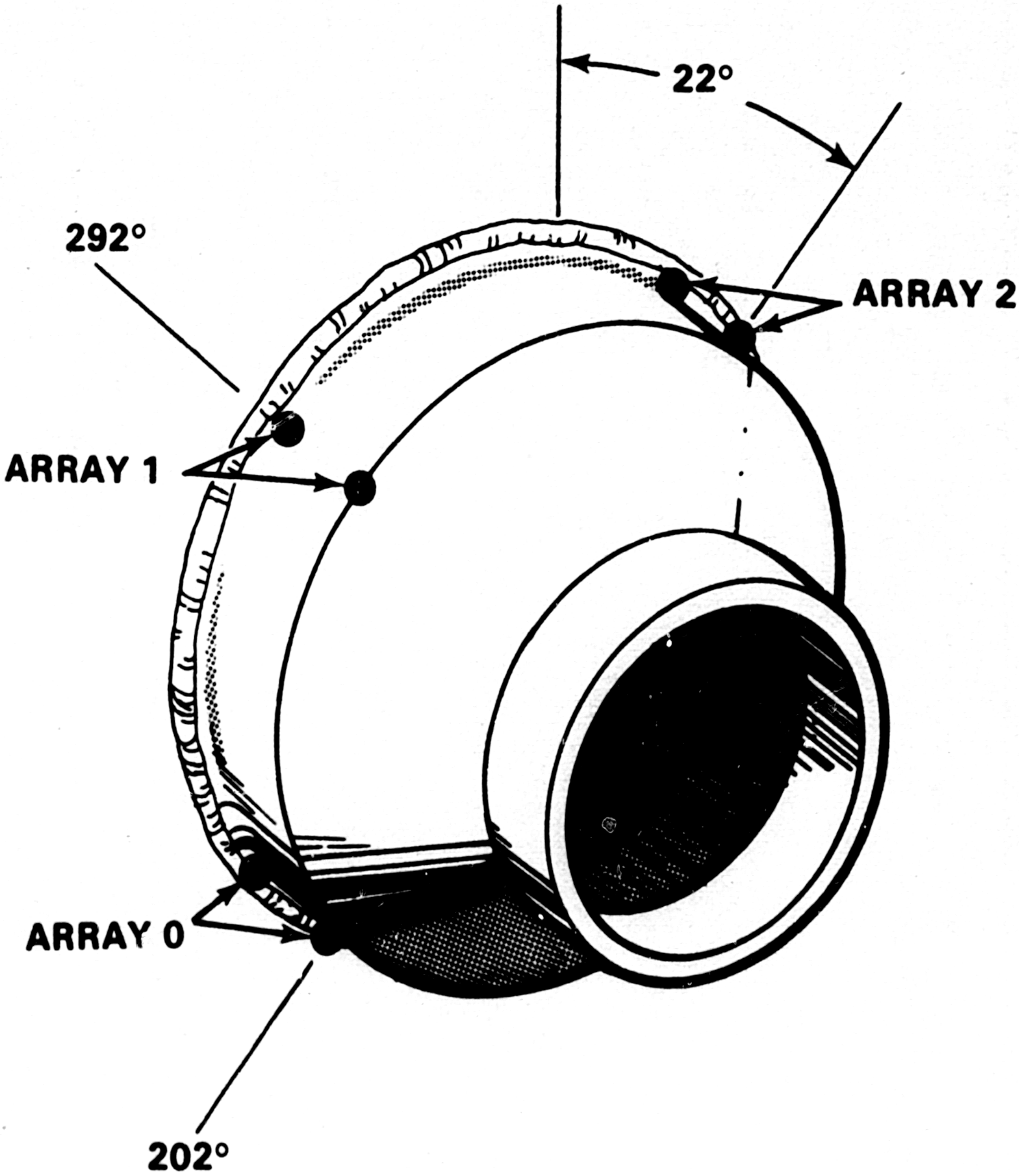

Figure 12. Location of AE Sensor Arrays on No. 2 Inlet Nozzle.

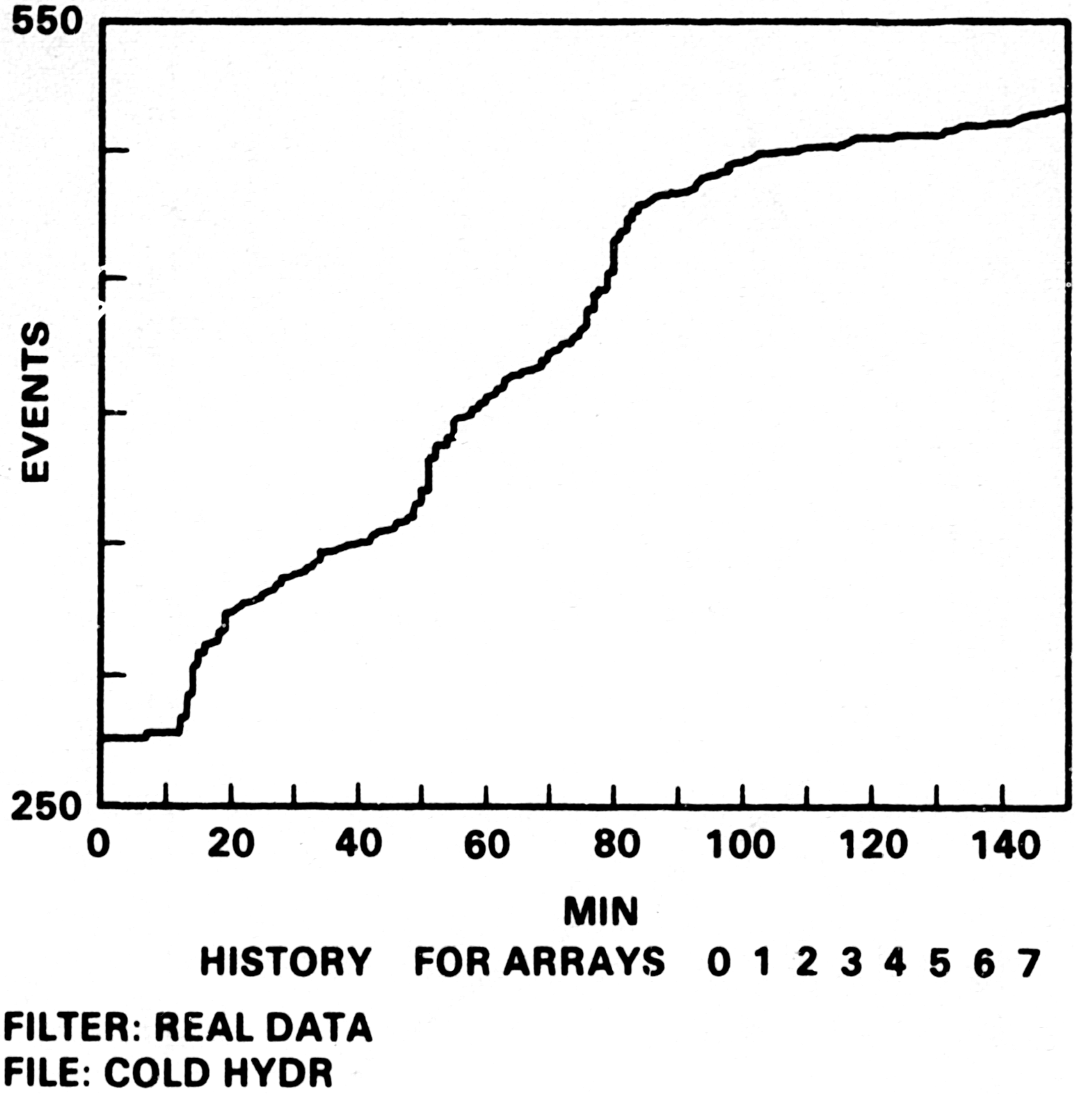

Figure 13. Filtered Events Versus Time for Final Pressure Gradient to Test Pressure.

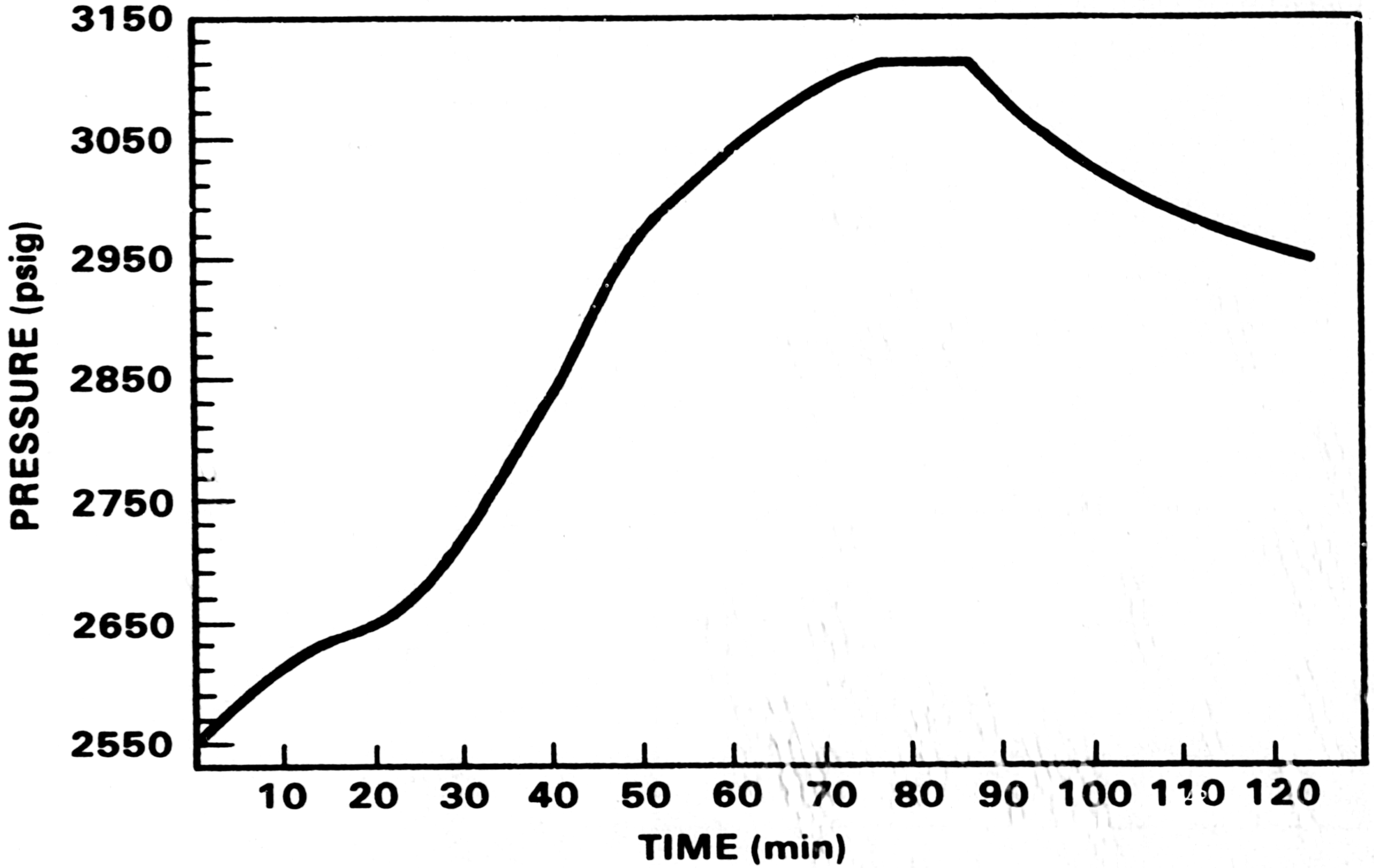

Figure 14. Pressure Versus Time Plot for Pressurization from Design to Test Pressure.

15) that the number of counts at array 1 was high relative to arrays 0 and 2. In order to determine possible sources for the acoustic emission activity observed, results from the fabrication and preservice examinations were correlated with the observed AE data. Figure 16 shows the location of preservice indiction in relation to array location. As can be seen by Figure 16 there are several slag indications that could account for the acoustic activity seen at array 1. The difference in time of signal arrivals at the array 1 sensors together with radiographic inspection results provide evidence that about half of the AE was originating from the defect at 306° nearest the array and the rest was from scattered sources. Examination of radiographs taken in the vicinity of the flaw gave the appearance that it was a slag inclusion about 1/4 inch in diameter located near the mid-wall position.

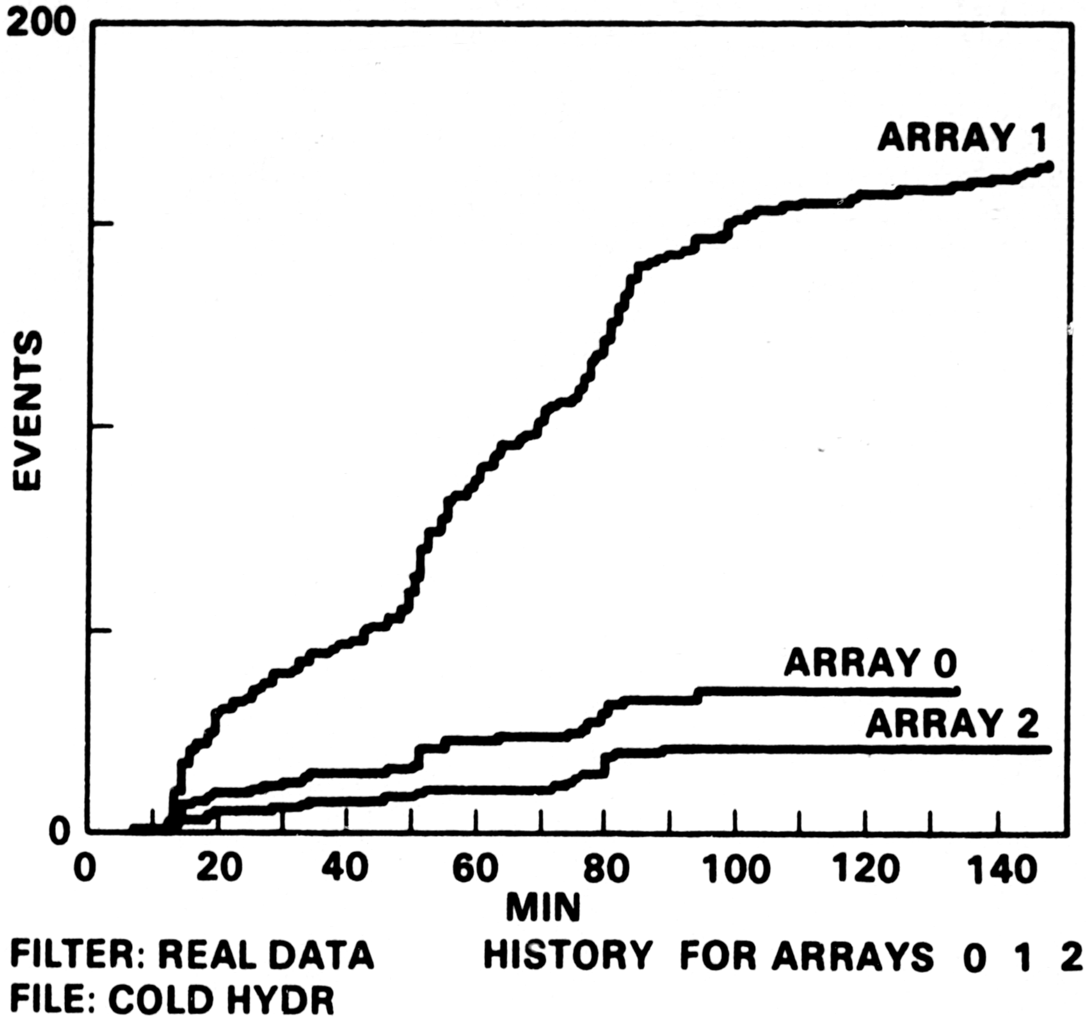

Figure 15. AE Data from No. 2 Inlet Nozzle Arrays During Final Pressure Ascent.

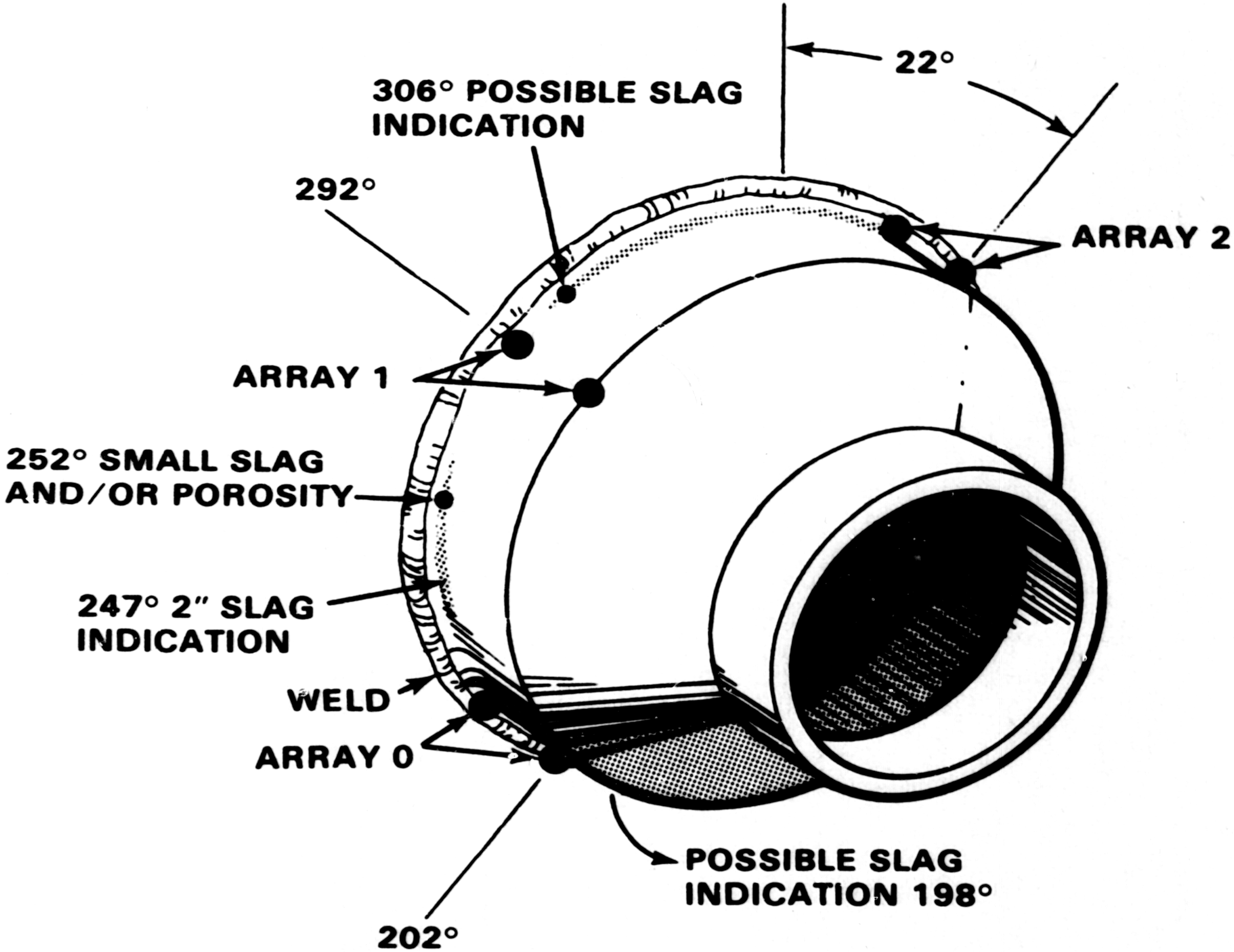

Figure 16. AE Sensor Arrays and Preservice Flaw Indications - No. 2 Inlet Nozzle.

6.0 ANALYSIS

The information derived concerning the unique response of AE sensor array 1 on the No. 2 inlet nozzle has been analyzed in two ways. One utilizes an AE/flaw evaluation technique developed under the NRC AE program and the other utilizes Code accepted flaw evaluation procedures. The objective is to make a first assessment of how the AE/flaw evaluation relationship compares with Code accepted procedures in a real field circumstance. It is very important at this point to bear in mind that this assessment has no implication as to the correctness of Code evaluation procedures; it is totally a first look at how the AE/flaw evaluation relationship responds to actual field information.

The flaw evaluation procedures of Section XI are based on the concepts and principles of linear elastic fracture mechanics (LEFM). The potential application of AE to flaw assessment, described here, is also based on LEFM using Section XI, Appendix A, as a foundation for developing the method of application.

To relate AE to the stress intensity factor, K_I, during hydrotest requires that experimental AE-K_I data exist for the relevant material conditions anticipated during pressure vessel service. This implies that the influence of environmental and loading conditions upon the material--and, hence, the AE response from that material--are known. Data from surface notch flaws in 6-in. thick A533B, Class 1 steel vessel hydrotests have been obtained and are shown in Figure 17 in terms of AE event count versus K_I.[3,4] These data, while showing the positive potential for vessel flaw assessment by AE, represent a limited data base for flaw severity assessment. Only a limited range of test conditions are represented by the curves shown in Figure 17. Nevertheless, a concept for a quantitative flaw evaluation procedure during hydrotest can be delineated from the vessel test data.[5]

The stress intensity factor resulting from a stressed flaw in a reactor pressure vessel during a hydrotest may be expressed as:

$$K_I = C_1 P_h \tag{1}$$

where P_h is the maximum hydrotest pressure and C_1 is a constant that includes flaw and vessel geometry terms and structural loading (e.g., conversion of pressure to stress) type factors. Equation (1) may be rearranged to yield:

$$K_I = C_1 P_o + C_1(P_h - P_o) \tag{2}$$

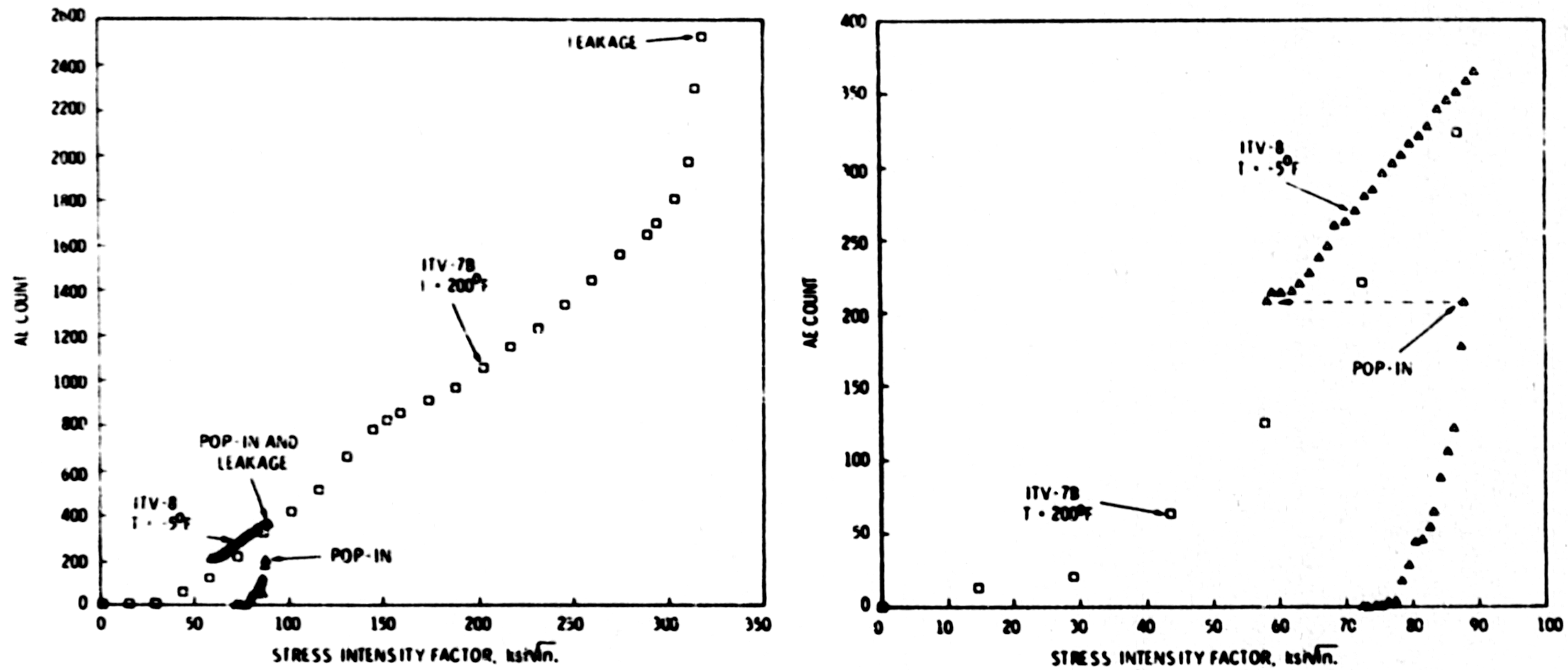

Figure 17. AE Data Obtained During HSST Vessel Tests V-7B and V-8.

where P_o is the nominal reactor operating pressure.

Figure 18 shows a hypothetical AE versus test pressure curve for a hydrotest. The number of AE count obtained from a particular flaw during the hydrotest, δN, may be used in conjunction with the data in Figure 17 to determine the change in stress intensity factor, δK_I, of the flaw due to changing the pressure from P_o to P_h.

The change in stress intensity factor due to the overpressure of the hydrotest is given as the second term in Equation (2) or:

$$\delta K_I = C_1(P_h - P_o) \tag{3}$$

Hence, for a particular quantity of AE from a flaw at a given location, that relation can be expressed:

$$\delta N = f(\delta K_I) \tag{4}$$

where $f(\delta K_I)$ represents the mathematical relationship for the flaw severity-AE data shown in Figure 17. Over the range of expected values for K_I (i.e., 15-200 ksi$\sqrt{\text{in.}}$), this relationship may be taken as an equation of the form:

$$\delta N = C_2 \delta K_I \tag{5}$$

where C_2 is the slope of the nearly linear relationship between AE and K_I.

Substituting the right hand side of Equation (3) into Equation (5) produced:

$$\delta N = C_2 C_1 (P_h - P_o) \tag{6}$$

Solving for C_1 and substituting back into Equation (1) produces an estimate of K_I at the hydrotest pressure level:

$$K_I = \frac{\delta N}{C_2} \frac{P_h}{P_h - P_o} \tag{7}$$

The maximum stress intensity factor (K_{max}) for operational pressure loading is then given as:

$$K_{max} = \frac{\delta N}{C_2} \frac{P_o}{P_h - P_o} \tag{8}$$

This flaw evaluation methodology was used with AE data obtained from array 1 on the No. 2 inlet nozzle. The most acoustically active region of the pressure vessel was the No. 2 inlet nozzle. During the final ascent in pressure, array 1

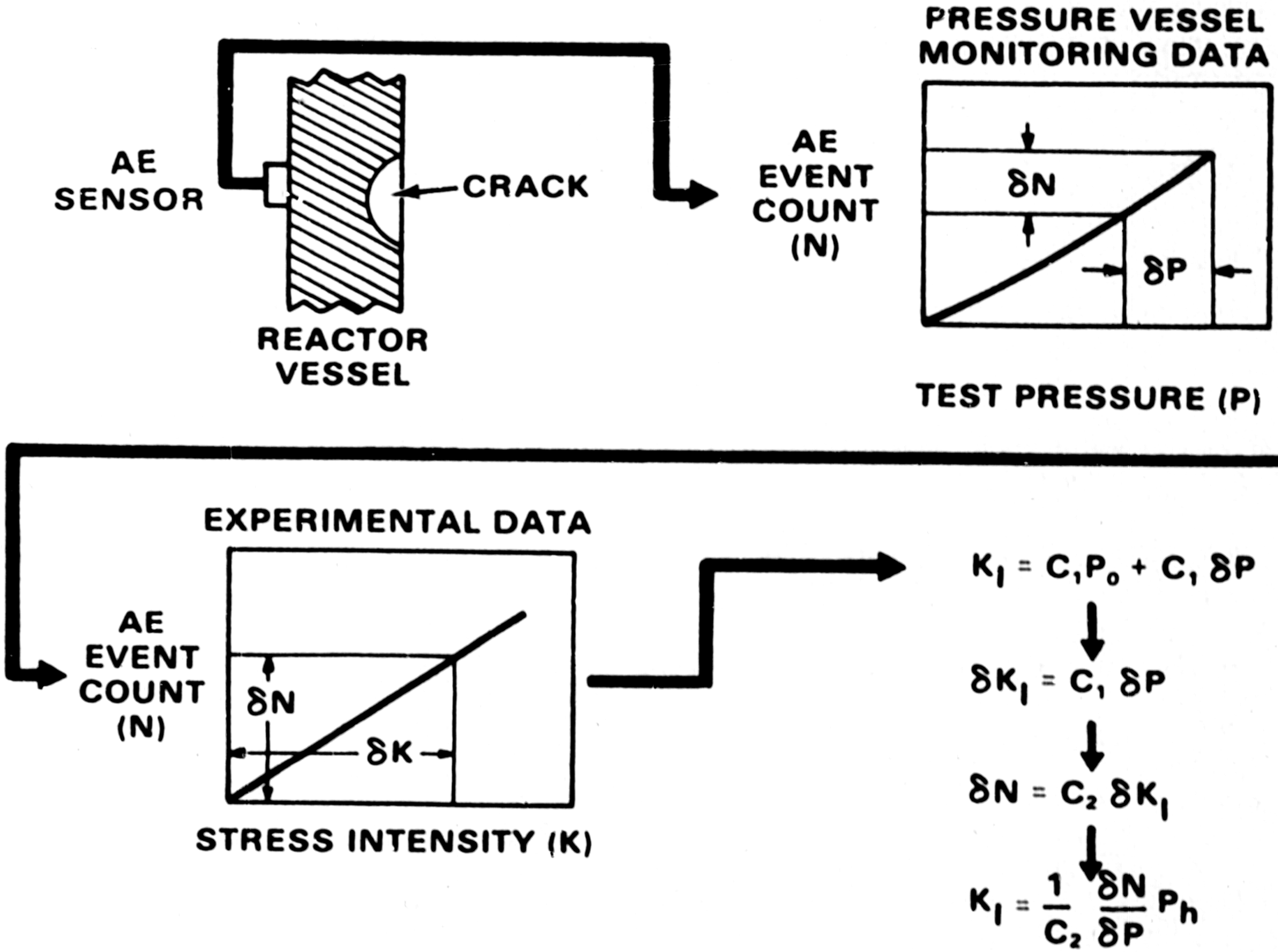

Figure 18. Method for Flaw Severity Estimate During Hydrotest.

recorded a total of 175 AE events. Detailed analysis of these 175 events indicated that 87 were from a definable material volume, but the remainder appear to have originated from widely divergent locations. Subsequent review of NDI (ultrasonic and radiographic) results shows an indication that appears, by location and by delta time of signal arrival at the AE sensors, to be the source of the AE data. Assuming the 87 signals may be considered as originating from a single defect, then an estimate of the maximum stress intensity factor for operating conditions may be obtained by inserting the following numbers into Equation (8):

$$\delta N = 87 \text{ events}$$

$$\delta P = 530 \text{ psi} = P_h - P_o$$

$$P_o = 2200 \text{ psi}$$

$$C_2 = 6.5 \text{ events/ksi}\sqrt{\text{in.}} \quad \text{(estimated from Fig. 17)}$$

$$K_{max} = \left(\frac{87}{6.5}\right)\left(\frac{2200}{530}\right) = 55.6 \text{ ksi}\sqrt{\text{in.}}$$

From examination of radiographs of the flaw area, it was deduced that the flaw is a slag inclusion approximately 1/4 in. in diameter and is located near the mid-wall position. Assuming that the flaw indication may be represented as a circular defect, then the stress intensity factor during hydrotest may be determined using the rules and procedures given in Section XI, Article A-3000 of the ASME Code.[6]

An estimate of the stress experienced in the nozzle blend radius during hydrotest was obtained from a paper by Riccardella and Mager.[7] The pressure vessel and nozzle geometry analyzed in Ref. (7) was the same as the Watts Bar reactor. From that analysis, the membrane, σ_m, and bending, σ_b, stresses were determined to be:

$$\sigma_m = 54.9 \text{ ksi}$$

$$\sigma_b = 26.9 \text{ ksi}$$

The stress intensity factor equation from Ref. (6) was given as:

$$K_I = \sigma_m M_m \sqrt{\frac{\pi a}{Q}} + \sigma_b M_b \sqrt{\frac{\pi a}{Q}} \qquad (9)$$

where a is the half-diameter of the embedded circular flaw, Q is the flaw shape parameter, and M_m and M_b are the membrane and bending stress correction factors, respectively. From Figures A-3300-1, A-3300-2 and A-3300-4 in Ref. (6) the following values for Q, M_m, and M_b were obtained:

$$Q = 2.26$$
$$M_m = 1.002$$
$$M_b = 0.023$$

Substituting these numbers into equation (9), taking a = 0.125 in. yields:

$$K_{max} = (54.9)(1.002)\sqrt{\frac{\pi(0.125)}{2.26}} +$$

$$(26.9)(0.023)\sqrt{\frac{\pi(0.125)}{2.26}} = 23.4 \text{ ksi}\sqrt{\text{in.}}$$

Recall, the value of K_{max} determined from the AE data via equation (8) is 55 ksi$\sqrt{\text{in.}}$. We find this encouraging even though the difference in K_I values is significant (fatigue crack growth rate has a power law relation to ΔK). The calibration of the AE/flaw evaluation relationship we are expecting here is whether it yields an answer that agrees fairly well with the Code (factor of 2 or 3 or less) or whether the result is in error by perhaps one or more orders of magnitude. Considering the uncertainties of the AE data (no point source location, no pattern recognition processing, and possible variations in response of AE systems), we do not feel it is productive to analyze these results any further.

7.0 CONCLUSIONS

AE monitoring the cold hydrostatic test of Watts Bar, Unit 1 produced results encouraging to achieving effective AE monitoring of nuclear reactor systems and it also identified areas where improvement in methodology is required.

The primary encouraging results are:

- AE produced by crack growth in a specimen attached to the safety injection pipe to No. 2 cold leg was detected.
- Spontaneous AE was detected from the No. 2 inlet nozzle during final pressurization.
- Preservice NDI information showed an indication (acceptable under the Code) which matched AE source indications.
- Evaluation of the flaw in the No. 2 inlet nozzle using an AE interpretation relationship agreed with a factor of two with an evaluation by ASME Section XI Code procedures.

Some areas where improvement in methods must be achieved are:

- Improved control of interference from background noise.
- Substantiation of AE sensor array configurations that are most effective in monitoring known areas of interest.

Items to be evaluated for improved background noise discrimination include modification of sensor tuning and use of a higher monitoring frequency. The true magnitude of the noise problem will not be clearly defined until measurements can be made with the core structure in place.

Two approaches to substantiation of optimum sensor arrays are being investigated. One is to arrange for access to a full scale nozzle mockup at the Electric Power Research Institute NDE Center to test nozzle monitoring. The second is to test the vessel wall monitoring array by arranging access to the inside of the Watts Bar Unit 1 vessel prior to installation of core structure. Both approaches obviously involve injecting artificial pulse signals to test AE system detection.

In conjunction with TVA construction forces, we are proceeding with installation of permanent signal leads to facilitate AE monitoring during hot functional testing and during reactor operation. The same locations described in this report will be monitored.

A final item of much significance to attaining effective monitoring is the knowledge to be gained from forthcoming AE monitoring of a vessel test in Germany. This test will involve both cyclic fatigue loading and hydrostatic test loading to various levels from 1.0 to 1.5 times operating pressure. The test period is expected to be 3 to 4 months. We feel this test will provide invaluable guidance to many aspects of effective reactor system monitoring.

REFERENCES

1. P. H. Hutton, "Summary Report on Investigation of Background Noise at the San Onofre Nuclear Power Reactor as Related to Structural Flaw Detection by Acoustic Emission," Battelle Northwest, July 1971, published in Southwest Research Institute Project 17-2440, Biannual Progress Report No. 6, Vol. I, Projects I through IV, January 7, 1972.

2. J. R. Smith, G. V. Rao and J. Craig, "Acoustic Monitoring Systems Tests at Indian Point Unit 1," COO/2974-2, Westinghouse Electric Corp., December 1979, NTIS, PC A06/MF A01.

3. G. D. Whitman and R. H. Bryan, "Heavy Section Steel Technology Program, Quarterly Report for July-September, 1977," NUREG/CR-0206, ORNL-TM166, April 1978.

4. R. H. Bryan, et al., "Test of 6-in.-Thick Pressure Vessels. Series 3: Intermediate Test Vessel V-8," U.S. Nuclear Regulatory Commission, NUREG/CR-0675, March 1980.

5. Pacific Northwest Laboratory, "Reactor Safety Research Programs, Quarterly Report October - December, 1979," NUREG/CR-1349, PNL-3040-4, pp. 83-87. August 1980.

6. Section XI, Appendix A, ASME Boiler and Pressure Vessel Code, 1977 Edition.

7. P. C. Riccardella and T. R. Mager, "Fatigue Crack Growth Analysis of Pressurized Water Reactor Vessels," ASTM STP 513, 1972, pp. 260-279.

APPENDIX I

DESCRIPTION OF DUNEGAN/ENDEVCO DATA ACQUISITION SYSTEM

APPENDIX I

DUNEGAN/ENDEVCO 1032D DATA ACQUISITION SYSTEM DESCRIPTION

PURPOSE OF EQUIPMENT

The Acoustic Emission Data Acquisition System is a multichannel system which can be used as a real-time system or as a stand alone unit for monitoring of acoustic emission activity for structural integrity assessment. This microprocessor based system, which may include up to 32 separate monitoring channels, can be used to gather acoustic emission information for evaluation during real-time operation. Recorded data can then be analyzed using a 1032D system wherever located. In this way, the analysis capabilities of the 1032D can be used to present recorded data. In addition to source location (planar, linear, cylindrical and spherical), the event attributes of amplitude, risetime, counts, and pulse duration may be used to provide plots of: time history, distribution functions, and correlations with external parameters or one of the other attributes. Filter parameters (windows) can also be set with the 1032D system for further characterization of the source data.

EQUIPMENT DESCRIPTION

The Acoustic Emission Data Acquisition System used at Watts Bar was configured as follows (see Figure I-1 for system block diagram):

1) D/E Model 6001 data acquisition system controller and interface.

2) D/E Model 6002 dual signal processor boards.

3) D/E Model 1111 system power supply.

4) Video terminal.

5) Model 74 Interdata computer.

The entire system, except for the video terminal and amplifiers, is housed in two 19-inch rack cabinets with casters. The major hardware items in a standard acoustic emission data acquisition system, and optional equipment, are discussed briefly in subsequent paragraphs.

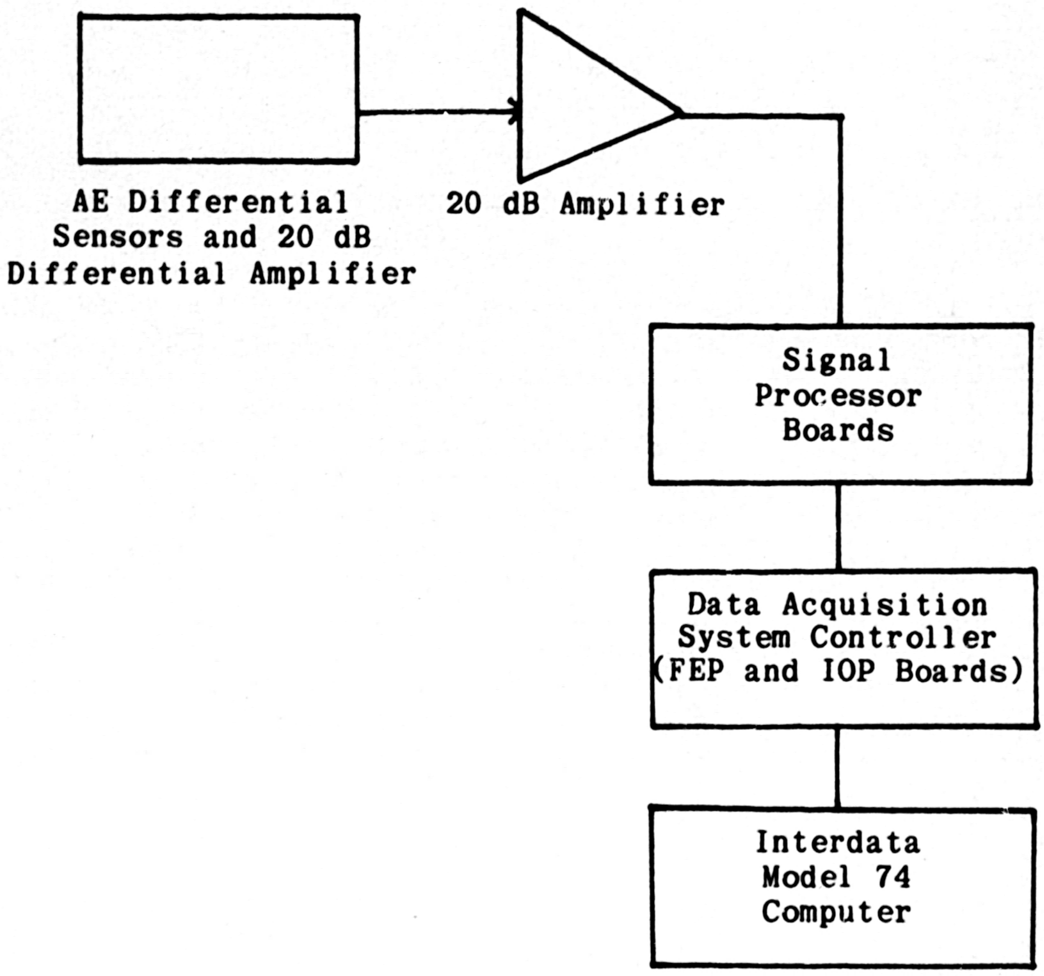

Figure I-1. System Block Diagram.

Data Acquisition System Controller and Interface

The Model 6001 data acquisition system controller and interface (DASCI) unit is an assembly with slots for 20 circuit boards (cards) and motherboard with connectors for interconnecting the circuit boards. One spare slot is allocated for extender board storage. The left most sixteen circuit board slots are reserved for signal processor (SP) circuit boards. Each signal processor board provides signal conditioning for two channels, permitting a total of 32 channels of signal processing in each data acquisition system controller and interface. If less than the full complement of 16 signal processor boards are used, the boards occupy the rightmost available slots, 16, 15, 14, ..., etc.

A front end processor (FEP) circuit board plugs into the 17th slot. The board has a full-function microprocessor which is dedicated to operating the sixteen signal processor boards and controlling event data transmission to the input/output processor board.

The input/output processor (IOP) board in slot 19, like the FEP board, is also microprocessor based. This board has primary functions associated with acquiring real-time event data from the FEP and from its own analog-to-digital inputs, buffering up to 500 incoming events, and providing formatted output to the Model 74 minicomputer with interactive control.

Power Supply

A power supply for the data acquisition system controller and interface is housed in a rack mounted assembly. This supply can be connected to either 115 VAC 50 Hz or 60 Hz power as specified. (Systems adapted, at the factory, to operate from a 200 VAC 50/60 CPS source, transform the higher voltage down to the 115 VAC range.) The output voltages and control signals are connected to the data acquisition system controller and interface chasses.

The unit uses a Pioneer Magnetics PM267A-1-4 switching power supply which provides up to 600 watts of dc output in multiple voltages. The outputs are:

+5 volts	40 amperes
+15 volts	10 amperes
-15 volts	10 amperes
+28 volts	3 amperes

NOTE: The ampere ratings are maximum for each channel. The power supply cannot have all channels operating simultaneously at full maximum.

Noise isolation of the switching portion of the power supply is provided by a heavy EMI filter which prevents switching regulator noise from being coupled out to the main power lines. This filter also serves to filter out incoming noise on the main power lines, effectively isolating the data acquisition system controller and interface from line noise.

DATA ACQUISITION

Data acquisition is performed by the data acquisition system controller and interface. It measures all data of interest relating to each acoustic emission event, stores the information temporarily in a buffer memory, and then outputs it in proper format to the permanent storage medium. For each event on each channel, the following signal attributes are measured: (1) counts; (2) peak amplitude; (3) average signal level; (4) duration; and (5) risetime.

NOTE: Relative time measurements of first threshold crossing (FTC), peak, and end of event (EOE) are made and later processed in the FEP and IOP boards to give delta-T's (based on FTC or peaks), risetime, and duration.

The time of occurrence of the event was determined from the time of first threshold crossing (FTC).

The data acquisition system controller and interface allows selection of a fixed or automatic threshold for event signal detection on a per-channel basis. The automatic threshold was used with the threshold set at 0.5 volts above background.

APPENDIX II

FREQUENCY SPECTRUM MEASUREMENTS

APPENDIX II

FREQUENCY SPECTRUM MEASUREMENTS

The frequency spectrum measurements presented in this paper were made by normalizing the frequency response from a helium jet calibration input with the background frequency response recorded during testing. The helium jet calibration at 30 psig was performed with the same set of amplifiers and cable lengths as were used during testing (i.e., care was taken to reproduce as closely as possible conditions that existed during testing). A flow diagram of the calibration system is shown below.

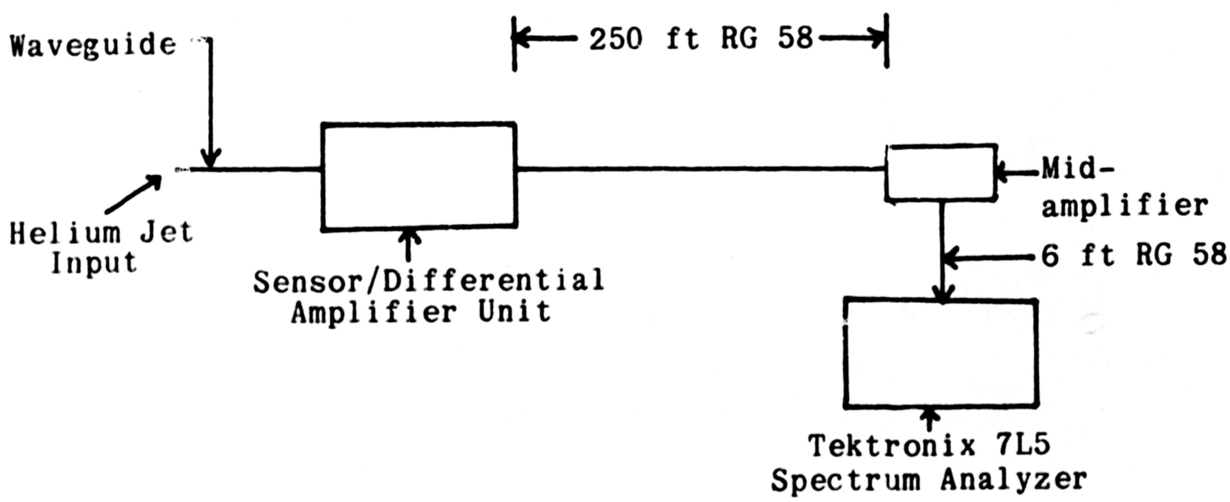

Figures II-1 and II-2 show the frequency response of the sensor amplifier combination used on the reactor to calibration and background noise input.

The following normalization procedure was used to calculate the normalized spectra in Figures 3 and 4 of the report text.

Spectra A (in II-1 and II-2) represents the frequency response with helium excitation at 30 psig.

Spectra B (in II-1 and II-2) represents the frequency response at the reactor vessel with all coolant pumps operating.

Normalized response in dB = Spectra B - Spectra A.

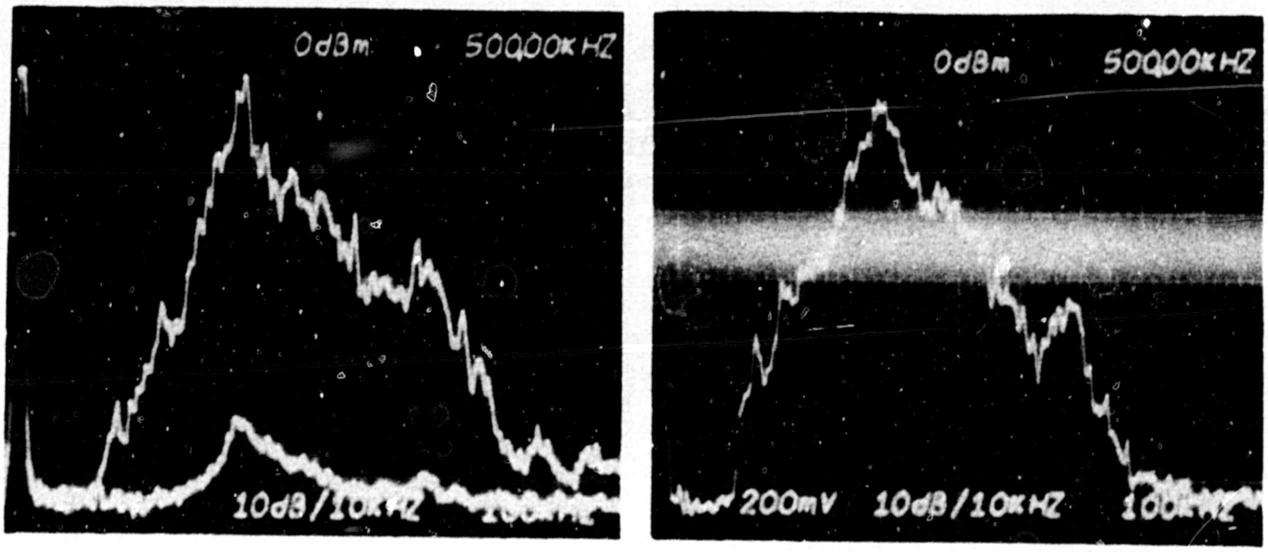

A B

Figure II-1. Helium Jet Calibration (A) and Background Noise at Nozzle (B).

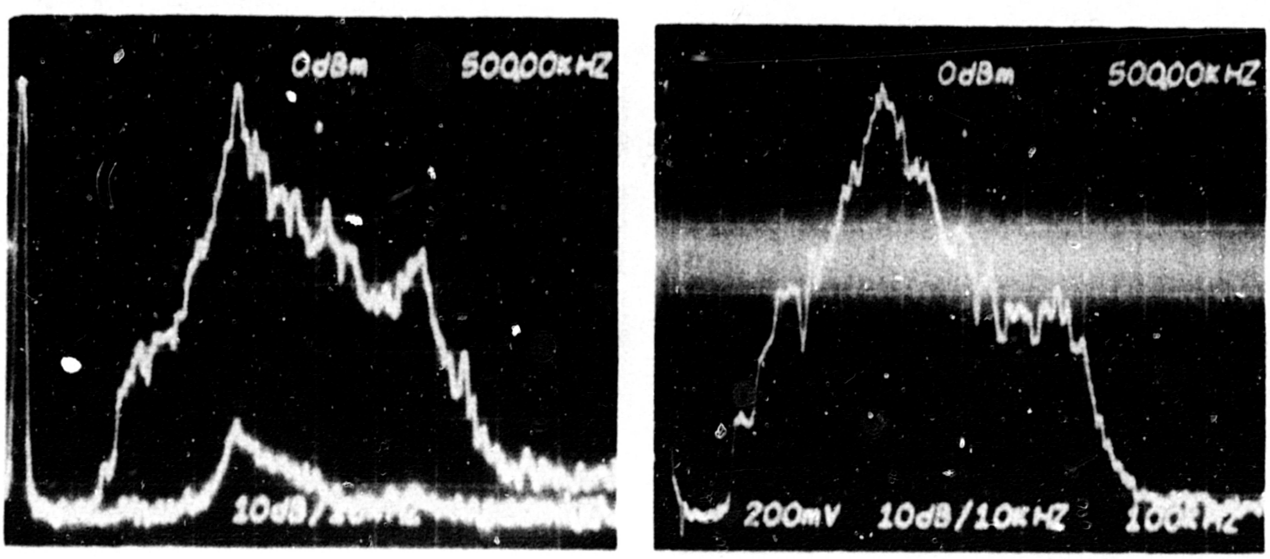

A B

Figure II-2. Helium Jet Calibration (A) and Background Noise at Accumulator Injection Pipe (B).

DISTRIBUTION

No. of
Copies

OFFSITE

A. A. Churm
DOE Patent Division
9800 S. Cass Avenue
Argonne, IL 60439

472 U.S. Nuclear Regulatory Commission
Division of Technical Information and Document Control
7920 Norfolk Avenue
Bethesda, MD 20014

2 DOE Technical Information Center

R. F. Abbey, Jr.
U.S. Nuclear Regulatory Commission
Office of Nuclear Regulatory Research
1130-SS
Washington, DC 20555

S. Fabic
U.S. Nuclear Regulatory Commission
Office of Nuclear Regulatory Research
1130-SS
Washington, DC 20555

R. B. Foulds
U.S. Nuclear Regulatory Commission
Office of Nuclear Regulatory Research
1130-SS
Washington, DC 20555

No. of
Copies

J. T. Han
U.S. Nuclear Regulatory Commission
Office of Nuclear Regulatory Research
1130-SS
Washington, DC 20555

D. A. Hoatson
U.S. Nuclear Regulatory Commission
Office of Nuclear Regulatory Research
1130-SS
Washington, DC 20555

T. Lee
U.S. Nuclear Regulatory Commission
Office of Nuclear Regulatory Research
1130-SS
Washington, DC 20555

G. P. Marino
U.S. Nuclear Regulatory Commission
Office of Nuclear Regulatory Research
1130-SS
Washington, DC 20555

J. Muscara
U.S. Nuclear Regulatory Commission
Office of Nuclear Regulatory Research
5650NL
Washington, DC 20555

No. of Copies		No. of Copies	
	C. Z. Serpan U.S. Nuclear Regulatory Commission Office of Nuclear Regulatory Research 5650NL Washington, DC 20555		G. Weidenhamer U.S. Nuclear Regulatory Commission Office of Nuclear Regulatory Research 1130-SS Washington, DC 20555
	M. L. Picklesimer U.S. Nuclear Regulatory Commission Office of Nuclear Regulatory Research 1130-SS Washington, DC 20555	15	John A. Raulston Chief Nuclear Engineer W10C126 Attn: Mr. E. A. Merrick,W3D194 Tennessee Valley Authority 400 West Summit Hill Drive Knoxville, TN 37902
	H. H. Scott U.S. Nuclear Regulatory Commission Office of Nuclear Regulatory Research 1130-SS Washington, DC 20555		
	W. Silberberg U.S. Nuclear Regulatory Commission Office of Nuclear Regulatory Research 1130-SS Washington, DC 20555		
	M. Vagins U.S. Nuclear Regulatory Commission Office of Nuclear Regulatory Research 1130-SS Washington, DC 20555		
	R. Van Houton U.S. Nuclear Regulatory Commission Office of Nuclear Regulatory Research 1130-SS Washington, DC 20555		

ONSITE

No. of Copies	
20	Pacific Northwest Laboratory
	J. F. Dawson P. H. Hutton (3) R. J. Kurtz D. K. Lemon R. P. Marshall R. B. Melton R. A. Pappas G. J. Posakony J. R. Skorpik A. M. Sutey T. T. Taylor Technical Information (5) Publishing Coordination (2)

NRC FORM 335 (7-77)

U.S. NUCLEAR REGULATORY COMMISSION

BIBLIOGRAPHIC DATA SHEET

1. REPORT NUMBER *(Assigned by DDC)*	NUREG/CR-2880
4. TITLE AND SUBTITLE *(Add Volume No., if appropriate)*	Acoustic Emission Monitoring of ASME Section III Hydrostatic Test - Watts Bar Unit 1 Nuclear Reactor
2. *(Leave blank)*	
3. RECIPIENT'S ACCESSION NO.	
7. AUTHOR(S)	P.H. Hutton, T.T. Taylor, J.F. Dawson, R.A. Pappas, R.J. Kurtz
5. DATE REPORT COMPLETED	MONTH July YEAR 1982
9. PERFORMING ORGANIZATION NAME AND MAILING ADDRESS *(Include Zip Code)*	Pacific Northwest Laboratory Battelle P.O. Box 999 Richland, WA 99352
DATE REPORT ISSUED	MONTH October YEAR 1982
6. *(Leave blank)*	
8. *(Leave blank)*	
12. SPONSORING ORGANIZATION NAME AND MAILING ADDRESS *(Include Zip Code)*	U. S. Nuclear Regulatory Commission Engineering Technology Division Office of Nuclear Regulatory Research Washington, D. C. 20555
10. PROJECT/TASK/WORK UNIT NO.	
11. CONTRACT NO.	Fin No. 2088
13. TYPE OF REPORT	Topical
PERIOD COVERED *(Inclusive dates)*	October 1981
15. SUPPLEMENTARY NOTES	
14. *(Leave blank)*	

16. ABSTRACT *(200 words or less)*

This report describes the acoustic emission monitoring performed during the ASME Section III hydrostatic testing of Watts Bar Nuclear Power Plant Unit 1 and the results obtained. Highlights of the results are:

- Spontaneous AE was detected from a nozzle area during final pressurization.
- Evaluation of the apparent source of the spontaneous AE using an empirically derived AE/fracture mechanics relationship agreed within a factor of two with an evaluation by ASME Section XI Code procedures.
- AE was detected from a fracture specimen which was pressure coupled to the 10-inch accumulator nozzle. This provided reassurance of adequate system sensitivity.
- High background noise was observed when all four reactor coolant pumps were operating.

Work is continuing at Watts Bar Unit 1 toward AE monitoring hot functional testing and subsequently monitoring during reactor operation.

17. KEY WORDS AND DOCUMENT ANALYSIS

17a. DESCRIPTORS

Acoustic emission monitoring reactor pressure boundaries for flaw detection

17b. IDENTIFIERS/OPEN-ENDED TERMS

Acoustic emission, continuous monitoring, flaw detection, reactor pressure boundaries

18. AVAILABILITY STATEMENT	Unlimited
19. SECURITY CLASS *(This report)*	Unclassified
20. SECURITY CLASS *(This page)*	Unclassified
21. NO. OF PAGES	
22. PRICE	$

NRC FORM 335 (7-77)

UNITED STATES
NUCLEAR REGULATORY COMMISSION
WASHINGTON, D.C. 20555

OFFICIAL BUSINESS
PENALTY FOR PRIVATE USE, $300

FOURTH CLASS MAIL
POSTAGE & FEES PAID
USNRC
WASH D C
PERMIT No. G67

120555078877 1 ANR5G5
US NRC
ADM DIV OF TIDC
POLICY & PUBLICATIONS MGT BR
PDR NUREG COPY
LA 212
WASHINGTON DC 20555

NUREG/CR-2880 ACOUSTIC EMISSION MONITORING OF ASME SECTION III HYDROSTATIC TEST OCTOBER 1982